REPUBLIC OF TÜRKİYE

ALTINBAŞ UNIVERSITY

Institute of Graduate Studies

Mechanical Engineering

MODELLING AND SIMULATION OF HIGH SPEED UNMANNED AERIAL VEHICLE

Aaya Sardar Qader DALLOO

Master's Thesis

Supervisor

Asst. Prof. Dr. Yaser ALAIWI

İstanbul, 2024

MODELLING AND SIMULATION OF HIGH SPEED UNMANNED AERIAL VEHICLE

Aaya Sardar Qader DALLOO

Mechanical Engineering

Master's Thesis

ALTINBAŞ UNIVERSITY

2024

The thesis titled MODELLING AND SIMULATION OF HIGH SPEED UNMANNED AERIAL VEHICLE Unmanned Aerial Vehicle prepared by SARDAR QADER DALLOO and submitted on 09/01/2024 has been **accepted unanimously** for the degree of Master of Science in Mechanical Engineering

____

Asst. Prof. Dr. Yaser ALAIWI

Supervisor

Thesis Defense Committee Members:

Asst. Prof. Dr. Yaser ALAIWI	Department of …, University	___________________
Academic Title First LAST NAME	Department of …, University	___________________
Academic Title First LAST NAME	Department of …, University	___________________

I hereby declare that this thesis meets all format and submission requirements for a Master's thesis.

Submission date of the thesis/dissertation to Institute of Graduate Studies: ___/___/___

I hereby declare that all information/data presented in this graduation project has been obtained in full accordance with academic rules and ethical conduct. I also declare all unoriginal materials and conclusions have been cited in the text and all references mentioned in the Reference List have been cited in the text, and vice versa as required by the abovementioned rules and conduct.

Aaya Sardar Qader DALLOO

Signature

ABSTRACT

MODELLING AND SIMULATION OF HIGH-SPEED UNMANNED AERIAL VEHICLE

DALLOO, Aaya Sardar Qader

M.Sc., Mechanical Engineering, Altınbaş University,

Supervisor: Asst. Prof. Dr. Yaser ALAIWI

Date: January / 2024

Pages: 59

Unmanned Aerial Vehicles (UAVs) have appeared as a pivotal industry in contemporary times, attributed to their adeptness at executing intricate tasks in both civilian and military domains without endangered human lives. Consequently, numerous researchers have passionately studied these aircraft. Especially under stringent and challenging conditions, to ascertain their structural integrity post-manufacture. The focal point of this thesis is an in-depth analysis of the Boeing X-45C aircraft, with particular emphasis on its fuselage. The aircraft will be meticulously designed and rendered using the SOLIDWORKS software, adhering to its authentic dimensions. After this design phase, the aircraft will be positioned within a precisely defined fluidic environment to facilitate a comprehensive CFD simulation using the ANSYS Fluent software, simulating the aircraft's flight at peak velocities. This will be followed by an FSI simulation, intertwining the insights gleaned from the CFD analysis with the potential ramifications on the aircraft's aluminium structure. The culmination of the thesis will present a thorough commentary on the results, evaluating the success and efficacy of the simulations and analyses conducted. The findings underscored the robustness of the aircraft, confirming its resilience under the tested conditions.

Keywords: FSI, CFD, UAV, Boeing, Design.

TABLE OF CONTENTS

Pages

LIST OF TABLES

Pages

LIST OF FIGURES

Pages

ABBREVIATIONS

UAV	:	Unmanned Aerial Vehicle
CFD	:	Computational Fluid Dynamics
FSI	:	Fluid-Structure Interaction
RMS	:	Root Mean Square
GCS	:	Ground Control Station
MSC	:	MacNeal-Schwendler Corporation
FEM	:	Finite Element Method
FEA	:	Finite Element Analysis

LIST OF SYMBOLS

ρ	:	Air Density
V	:	Velocity of the Object
L	:	Characteristic Length (Like Chord Length for Wings)
μ	:	Dynamic Viscosity of the Fluid
p	:	Pressure
g	:	Acceleration Due to Gravity
z	:	Elevation
LF	:	Lift Force
S	:	Wing Reference Area
C_L	:	Lift Coefficient
D	:	Drag Force
C_D	:	Drag Coefficient
u	:	Velocity Components in the X Directions
v	:	Velocity Components in the Y Directions.
w	:	Velocity Components in the Z Directions.
ν	:	Kinematic Viscosity of the Fluid.

1. INTRODUCTION

1.1 BRIEF BACKGROUND

Airplanes have transformed how we travel, do business, and engage with the world. Civil aircraft, covering all non-military planes, are central to this change. These planes fall into three main categories: private, business, and commercial airliners. Private planes are mostly for personal use, typically being single-engine monoplanes. Their variety is impressive, from the nostalgic "warbirds," which are former military planes, to "homebuilt" made by hobbyists from kits or from the ground up. There are also antique planes, lovingly restored relics of the past, and aerobatic planes, built for nimble manoeuvres and air show displays. Business planes have a commercial focus, bringing in revenue for their owners. They range from small single-engine aircraft used for short trips or training to grand four-engine jets that can travel across continents. These planes are especially valuable for top executives, allowing them to bypass regular airline schedules. They're versatile too, used for various tasks like farming, medical rescues, cargo transport, weather research, and even police operations. Sadly, some have been used for illegal purposes, like drug smuggling. Commercial airliners are built to carry passengers and cargo on set routes between chosen airports. They come in all sizes, from modest single-engine cargo planes to the massive Airbus A380. Their speeds vary too, from slower speeds to the rapid pace of the renowned Anglo-French Concorde, which graced our skies from 1976 to 2003. Overall, the wide array of civil aircraft has not just brought the world closer but has also boosted economies, fostered cultural ties, and spurred tech innovations [1].

The concept of Unmanned Aerial Vehicles (UAVs) was not conceived recently. It is revealed that the inception of UAVs took place during the challenging period of World War I. In the early 20th century, rapid technological advancements were being observed by the world. Among these advancements, the creation of aircraft that could function without an onboard human pilot was conceptualized. In 1917, the first attempts were made, with the main aim being the design of aircraft that could act as moving targets for antiaircraft gunner training. Radio-controlled aircraft were what these early UAVs essentially were, and their progression was considerably slowed by the technological constraints of that time. As World War II approached, a greater military potential of UAVs started to be recognized. The potential of utilizing these pilotless aircraft as assault drones was particularly seen by the US Navy.

These drones were not just envisioned as mere targets but were also considered for real combat situations. For example, during the Bougainville campaign in 1944, the TDR-1 drones were employed as guided missiles. However, it's crucial to understand that these weren't Unmanned Combat Air Vehicles (UCAVs) as known today. They resembled kamikaze aircraft more closely, designed for a single mission without the ability to return to base post-mission. The period following the war, especially the Cold War, signified a notable transition in UAV development and utilization. The emphasis shifted from drones being used as assault tools to their deployment for reconnaissance. In the 1950s, the US Army's growing interest in this domain was evident. Existing target drones were modified by them, fitting them with cameras to act as aerial observers over battlefields. The SD-1 drone, which was modelled on the Radio plane RP-71 target drone, was a notable initiative in this direction. This drone was launched using rocket-assisted take off, radar-tracked, completed its reconnaissance mission, and then was returned to base, where parachutes were used for its recovery. As years passed, significant technological transformations were witnessed. The latter half of the 20th century saw the introduction of digital cameras, advanced satellite navigation systems, and potent computer microprocessors, all of which drastically enhanced UAV capabilities. These technological advancements enabled UAVs to transition from mere aerial observers to multifunctional entities capable of surveillance and actual combat missions, equipped with precision-guided munitions. In summary, UAVs' history stands as a symbol of human innovation and the continuous drive for technological progression. From their initial role as moving targets for gunner training to their indispensable role in contemporary warfare, UAVs have undergone significant evolution. Their development reflects the broader progression of military technology, showcasing the evolving nature of warfare and the persistent human aspiration to outperform opponents[2].

1.2 UAVS TYPES

a. Multi-Rotor UAV: Multi-rotor drones represent the most user-friendly and economical choice for aerial photography and monitoring. Equipped with several rotors, their configurations can vary from Tri copters (3 rotors) to octocopters (8 rotors), with quadcopters being the most common. These drones provide exceptional manoeuvrability and framing precision, making them ideal for activities such as visual assessments, thermal imaging, photography, videography, and 3D mapping. However, their restricted endurance and speed render them less suitable for expansive aerial mapping or extended-range inspections [3].

Figure 1.1: Quadcopter it’s Type of Multi-Rotor UAV [4].

b. Single-Rotor Drones: Single-rotor drones resemble helicopters, featuring one main rotor along with a tail rotor. These drones are efficient, particularly when fuelled by gas, and can transport substantial loads. Their design permits the use of longer blades, which outperform regular propellers in efficiency. They excel in tasks like aerial LIDAR laser scanning, drone-based surveys, and transporting heavy items. However, they can be a bit complicated, cost more, and need consistent maintenance [3].

Figure 1.2: Single Rotor UAV [5].

c. Fixed-Wing Drones: Fixed-wing drones look like regular airplanes and are built for fuel efficiency. They can travel great distances, survey vast regions, and stay airborne for extended periods, even exceeding 16 hours when powered by a gas engine. These drones are perfect for tasks like aerial mapping, surveys in forestry and agriculture, inspections, construction, and security. However, they might be harder to operate, often needing proper training, and the data processing after their flights can be quite detailed [3].

Figure 1.3: Fixed Wing UAV [6].

d. Fixed-Wing Hybrid VTOL: These drones merge the advantages of fixed-wing and rotor-driven models. They feature rotors on their fixed wings, allowing them to hover and ascend or descend vertically. While they're still being refined, they show potential for uses such as drone deliveries. Amazon's Prime Air delivery drone is a notable example [3].

Figure 1.4: Fixed-Wing Hybrid VTOL UAV [7].

1.3 THESIS ORGANIZATION

In Chapter 1, a concise overview of aviation is provided, its significance is emphasized, and a thorough exploration of the history of unmanned aircraft is undertaken. The different classifications of these aircraft are then delved into.

In Chapter 2, the findings and insights from various researchers are showcased, with both general research on unmanned aircraft and specific studies focused on CFD analysis being highlighted.

In Chapter 3, the principles of aerodynamics and the specifics of CFD, including its equations, are unpacked. The notion of FSI is clarified. An aircraft is then designed, with inspiration drawn from standard market dimensions, and a detailed analysis of this design is provided.

In Chapter 4, the outcomes from the CFD analysis and the FCI are presented and discussed in depth.

In the final chapter, the key takeaways are summarized, and recommendations for future investigations in this field are put forward.

1.4 THESIS GOALS

The objectives of this thesis are to perform a conceptual fluid dynamic analysis on a well-known aircraft with dimensions that are placed within the scope of the market dimensions. Another goal is to clarify how the FSI analysis works for this type of aircraft very accurately, as well as to explain the importance of using more than one computerized software for the simulation process, for example here it will be The use of the SOLIDWORKS software for design and ANSYS workbench for analysis, and another goal of this thesis is to clarify the sciences of aerodynamics and CFD in a clear and detailed manner, as well as the FSI analysis and the importance of its results on the aircraft's path and safety.

2. LITERATURE REVIEW

A fixed wing unmanned aerial vehicle (UAV) was examined in a research study that was conducted, which was used for mapping semi-undulating regions. A slope-mapping method known as photogrammetry was assessed in the investigation. Images were captured at an elevation of 300 meters by the UAV that was deployed. Photogrammetry, a technique developed within the study, also referred to as Digital Orthophoto and Digital Elevation Model (DEM), was used to analyze all the collected images. The research findings indicated that the root mean square (RMS) error was 0.259 for length analysis and 1.169 for slope, demonstrating the practicality of this mapping approach [8].

The impact of vibration on the use of composite materials in the wings of unmanned aerial vehicles was focused on particularly in a previous study. The modal characteristics of the wing in two distinct setups were compared in the study: one where the wing was vertically mounted for shaker-table testing, and another where the wings were attached to a suspended UAV, simulating a free setup. Vibrational characteristics including natural frequencies, associated modes, and damping coefficients, were garnered via this study, with 16 biaxial accelerometers installed on both wings. Data collection both inside and outside the plane was allowed for by this particular accelerometer configuration, which was utilized to determine the shape of the situation. Significantly larger and less noisy signals compared to data acquired from a complete UAV configuration were yielded by the shaker-table method [9].

An analytical structure for a drone model to simulate the flight dynamics of a fixed-wing aircraft was proposed in an earlier study, which was incorporated into the dynamic model in the DATCOM software. A model was created using flight test data, which was experiment-based, and was effectively refined using a Kalman filter, contributing to the validation of the analytical model. Upon comparison of the two systems, dynamic models with comparable characteristics were yielded, as was discovered [10].

An unmanned aircraft's carbon composite wing was investigated in a previous study which discussed the properties, rigidity, and strength. This lightweight aircraft's wing was constructed using multiple ply patterns of varied spars with different wall thickness dimensions and laminates. It also consisted of sandwich skins with a foam core. A three-tiered system known as the whiffletree system was designed and employed to appropriately load the wing under a pull-up maneuver condition. The wing's static response at various chordwise and spanwise locations was gauged using multiple deflection and strain gauges. Close alignment with experimental observations was found in predictions of deflection and stress, drawn from finite element simulations, indicating the wing's substantial strength despite its light weight [11].

Composite materials for unmanned aircraft were simulated in other studies using the SOLIDWORKS software. Initially, the properties of composite materials broadly were examined, and then two specific instances of composite structures: laminates and sandwich composites were numerically analyzed. The differences in the primary pressures, P1 and P3, as well as displacement values within the analyzed structures, all under consistent boundary conditions were highlighted in the study. Additionally, the progression of the manufacturing process was elucidated [12].

A UAV built from composite materials was produced and tested in a previous study. The construction process for durable, lightweight UAVs was described, and the flight performance of such composite aircraft was assessed. Fiberglass composites were primarily employed in construction. Initially, Styrofoam was used to shape the aircraft. In the subsequent stage, one side of the aircraft was created by applying resin and fiberglass to the form. Remarkable stability and strength, particularly in terms of pitch and roll were demonstrated by the aircraft as per the flight test data [13].

The development of an automatic landing system for fixed wing unmanned aerial vehicles was discussed in a certain master's thesis. Location information computed by image-processing algorithms was used to conduct an automatic landing by this system. A Ground Control Station program, developed using the GCS software, was used to send commands to the autopilot for either performance analysis of landing, changing the location data source, or activating or deactivating pilot functions. The system was successfully tested in various flight environments and under different conditions of turbulence and wind, demonstrating the aircraft's automatic guidance capabilities [14].

The composite structures and material strength of a Belly-Landing Mini UAV were delved into by a previous investigation. The UAV's fuselage was designed and developed using materials for the research, with two-layer sandwich structures made from epoxy resin and composite materials. In line with the standard, three distinct forms of tensile test samples and strength test samples for the composite materials were fabricated. Carbon and glass fibers mixed with epoxy resin demonstrated excellent tensile strength and Young's modulus

as per the findings. Stresses were computed by carrying out a simulation utilizing Inventor software, and the results were promising, suggesting a highly safe design. Furthermore, the aircraft's success in both maneuvering and take-off tests was confirmed by flight trials [15].
In previous research, a control device for a small, fixed-wing UAV, designed to maintain a specific flight path in turbulent wind conditions, was discussed. The primary objective of the controller, to compensate for wind impact and maintain the intended flight trajectory, was confirmed to be theoretically globally asymptotically stable. This was followed by the performance of the controller being assessed through multiple simulations. The composite controller, incorporating a disturbance observer, was revealed to be stable and aligned well with the theoretical analysis, as per the outcomes. Initial flight trials yielded results that were positive and within acceptable parameters when the controller was put to the test [16].
An exploration, optimization, and design for a fixed-wing structure of an unmanned aircraft were undertaken in different research. A comparative analysis among various types of wings - specifically, the Beam type, Multi-Ventral-Plate, and Single Block Type, was carried out. The Beam type was concluded to be the superior choice after simulating under specific conditions, including a drag force of 50 Newtons and a lift force of 100 Newtons, suggesting enhancements to the fixed-wing UAV's design due to its efficiency [17].
This previous research undertook a comprehensive study of the design standards for an Unmanned Aerial Vehicle (UAV) system, specifically targeting a loiter munition UAV. This UAV system was designed to feature day and night functionality, a flight time between 2-3 hours, and the capacity for catapult launch. Additionally, the UAV was conceived to be compact, easily navigated via a personal Global Positioning System (GPS), and fitted with cutting-edge avionics, marking it as ideal for defense and border patrol activities. The UAV's structure, characterized by a mid-wing, dual-tail, and a relatively light frame, was found to provide stability across three axes. The research concluded that this design not only assures the UAV's steadiness but also offers notable cost benefits during operations [18].
The process of designing, analyzing, and fabricating a composite frame structure for an unmanned aircraft was narrated in the subsequent study. The structure comprises a lattice composite structure created using a 3D printer that operates with continuous carbon fiber, and two matrix materials, one of them being a thermoset. The 3D printing process and the finite element analysis of the structure were outlined in the study. A considerable correlation

between the experimental data and the theoretical predictions was demonstrated by the analysis results [19].

In a previous study, the simulation of a tubercle leading edge for an unmanned aircraft's wing, made from composite materials, using finite element methods was focused on. SOLIDWORKS software was utilized in the design phase, while the development of the finite element model utilized ANSYS software. The aim was to measure the impact of deformation and stresses on the composite wing of an unmanned aerial vehicle, particularly the tubercle at the wing's leading edge. The reinforced rib and the monocoque-foam were the two varieties of composite materials explored. The monocoque-foam considerably reduced deformation by 50.72% and stress by 35.88%, outperforming the reinforced rib, as per the results post-analysis [20].

A detailed method for the initial design of aircraft, highlighting the use of one-way fluid-structure interaction (FSI) in aircraft design, was presented. The main goal of the research was to refine the wing shape of an unmanned aerial vehicle (UAV) to achieve the lowest possible cruise drag. The design factors in focus were the wing's taper ratio and dihedral angle, with the UAV's cruise drag as the target outcome. By employing Fluid-Structure Interaction (FSI) analysis and optimization techniques, the aircraft's drag was reduced by 6.3%. The prediction model, crafted using the Kriging method, showed a 2.7% deviation in estimating the lowest drag. These results highlighted the value of FSI analysis in improving UAV design for better aerodynamic efficiency [21].

One of previous research paper, concentrates on the meticulous task of enhancing wing designs specifically for unmanned aerial vehicles (UAVs) with a focus on long-endurance capabilities. This scholarly work underscores the significance of employing Fluid-Structure Interaction (FSI) analysis in close coordination with the Kriging method to achieve its goals. The central aim of the study is to identify the most aerodynamically efficient wing shape, particularly one with a high aspect ratio, that would result in the minimum amount of aerodynamic drag when the UAV is in cruise conditions. To facilitate this complex optimization process, the research team utilized a specialized design optimization tool known as PIAnO. This software not only integrates seamlessly with proprietary codes for simulation and optimization but also serves multiple functions: it assists in the generation of various wing geometries, enables the efficient transfer of information between different stages of the design process, and aids in accurately identifying the most optimal wing shape based on the set criteria. Upon completion of their rigorous analysis, the researchers found that the most optimal wing configuration achieved a noteworthy reduction in drag. Specifically, the aerodynamic drag was reduced by 5.95% when compared to the initial wing design that served as the baseline for the study. Therefore, the study provides valuable insights and a practical approach to significantly improving the aerodynamic efficiency of long-endurance UAVs [22].

The application of composite materials in the construction of unmanned aircraft was shed light on by another study. The experimental characterization of a polymer matrix composite laminate, which incorporated an epoxy resin system fortified with graphene oxide (GO), in addition to fiberglass, was primarily focused on in this study. Upon reviewing the experimental results, it was observed that EPWM12 outperformed other laminates in terms of maximum tensile strength and ultimate tensile strength. The incorporation of graphene notably strengthened the epoxy composite, resulting in a 4.3% increase in the elongation value as compared to conventional epoxy. Moreover, the Young's modulus of the epoxy composite was found to be approximately 66% greater than that of regular epoxy, nearly a fourfold increase [23].

This past article underscores the growing importance of unmanned aerial vehicles (UAVs) because of their affordability and wide-ranging uses. Yet, there seems to be a gap in design techniques that encompass both aerodynamic and structural assessments for UAV propellers. In this study, a new approach was proposed for the aerodynamic crafting of propellers, utilizing advanced tools and parameters. This was paired with a structural assessment technique using the Finite Element Method (FEM). The research delved into various propeller designs using BEMT and MIL techniques. After finalizing the design through the specified process, it underwent detailed numerical tests. These tests combined aerodynamic forces with structural design, using Fluid-Structure Interaction (FSI) in ANSYS 18. The aerodynamic assessment revealed a close alignment between BEMT and CFD findings, with only a slight deviation. Additionally, certain propeller designs demonstrated superior thrust production. In summary, the research's main achievement was crafting a design technique for UAV propellers, aiming to forecast their efficiency and ideal designs in the initial design stages [24].

An detailed study focused on the design of a medium-range fixed-wing unmanned aerial vehicle (UAV) that can carry a 25 kg payload was introduced. The design of the wing underwent a Fluid-Structure Interaction (FSI) analysis to verify its design and improve its aerodynamic qualities. The value of FSI simulation was highlighted because it provides a cost-effective and quick way to evaluate aircraft performance, eliminating the need for repeated tests. The project involved defining flight criteria, examining UAVs with similar specifications, and employing a cyclical estimation method to determine the UAV's total takeoff weight. After evaluating several airfoils, the Wortmann fx-76-mp-140 was selected for the wing. A 3D model of the wing's structure was developed using SOLIDWORKS, and its design was confirmed with XFLR5 and FSI analysis. Insights regarding the lift to drag ratio, wing deformation, and stress were obtained from the FSI analysis done in ANSYS. After testing various configurations in dihedral angle, chord length, and wingspan, the study concluded that extending the wingspan from 4.61 meters to 5.11 meters resulted in a 4.9% improvement in the lift to drag ratio [25].

In previous research titled, the incorporation of the nonlinear structural tool MSC Nastran into a concurrent programming setting, Flow Simulator, was examined. The main goal was to enable fluid-structure interaction (FSI) assessments by merging fluid and structural analysis tools. The research presented a module-based framework where MSC Nastran functions as a central server, connecting with other modules through an XML-RPC server. This arrangement ensures smooth data transfer and coordination during joint analysis. The importance of MSC Nastran's OpenFSI interface was highlighted, as it allows for the integration of real displacement states from the fluid tool and the gathering of resulting loads for structural evaluation. The study pointed out two primary examples: one depicting a beam-like action that becomes rigid due to significant deflections and rotations, and another showing surface buckling on a slender-walled wing structure, influencing the overall rigidity and nearby airflow. Both examples revealed the shortcomings of traditional linear theory in identifying these nonlinear actions [26].

An evaluation of engine lifespan, specifically focusing on fatigue estimation in unmanned fixed-wing aircraft, was tackled in this study. A systematic approach was presented to forecast the lifespan of these engines, referred to as "gray color", particularly those functioning in high-stress conditions. Gray prediction models were utilized, drawing on output power decay data for a span of 50 flight hours. The study's results indicated that the engine's power decreases to 9.4 kilowatts under typical operation after 100 hours; a power level below this renders the aircraft incapable of completing its journey appropriately. In high-stress circumstances, these predictive models leveraged degradation data accumulated over 70 hours. The study concluded with a comparative analysis of the predictive results and methodology with alternative approaches such as autoregression, and it was determined that the gray prediction method was more precise [27].

Prior research delved into the design process of an unmanned aerial vehicle, utilizing CATIA V5 software for this purpose. Following this, the performance of the aircraft was scrutinized using ANSYS and XFLR software, providing insights into the aerodynamic properties of the fixed wing of the UAV. The goal was to augment the aerodynamic design of the aircraft in question. To extend the duration of the flight mission and achieve the highest possible altitude, the most favorable glide ratio was calculated. The simulation process was carried out using a Mach number of 0.04202, approximately equating to a speed of 14.3 meters per second. The aircraft's construction comprised composite materials like glass and carbon fibers [28].

Methods for simulating the nonlinear dynamics of fixed-wing UAVs under varying conditions of airspeed and flight altitudes, with the aim of developing a nonlinear adaptive controller, were explored in this previous study. The model was comprised of a 10-degree of freedom differential equations system that segregated the conditions of the aileron, throttle, rudder, and elevator from the constructed model. Simulations revealed the flight dynamics behavior of a specific aircraft used as the study subject, in this case, the Wulung UAV. The simulation results closely mirrored the data from actual flight tests [29].

The previous study examined the aerodynamic adjustments made to the RQ-7 Shadow's wing. The research scrutinized the implications of tweaking elements of the wing design, including the airfoil, shape, aspect ratio, and the addition of a winglet, particularly during the plane's ascent and acceleration stages. A primary goal was to determine the viability of high-lift airfoils, such as the EPPLER 559, for slower UAV uses. Using ANSYS FLUENT, five unique wing designs were assessed through Computational Fluid Dynamics simulations. The results indicated that, when compared to the NACA 4415 airfoil, the EPPLER 559 airfoil provides enhanced lift at reduced angles of attack. However, its advantages wane as the angle of attack increases. The research concluded that while the EPPLER 559 airfoil holds promise for slower UAV uses, its efficiency relies on specific adjustments in wing design elements [30].

In prior research, a detailed analysis of the mechanics of flapping wings, especially for Unmanned Air Vehicles (UAVs), was conducted. The growing need for compact UAVs, particularly for operations in challenging environments like urban settings, has highlighted the importance of understanding wing designs influenced by nature. The focus of the research was on creating and confirming a computational fluid dynamics (CFD) tool that combined a fluid-structure interaction (FSI) solver with vehicle control algorithms. This unified method aimed to forecast the efficiency of a sample flapping wing UAV. Wings inspired by nature, built with carbon fiber frameworks and flexible Mylar membranes, were studied. The combined solver was checked against standard scenarios, and the findings indicated its reliability and promise. Additionally, early simulations of pitch control movements revealed that the vehicle could return to the desired position in merely three wing flaps [31].

A structural analysis of an unmanned aircraft, specifically focusing on its wing composed of composite material, was conducted in previous research. The finite element method was utilized in this study, employing the ANSYS software to investigate and juxtapose a variety of laminates on the wing surface. Additionally, the benefits of using structural elements like ribs and spars were also explored in the study. The simulation revealed data about the degree of deformation, resistance, and potential failure under defined conditions. The analytical results indicated that the optimal load reduction was achieved by varying the distributed load along the pressure center. The most effective surface lamination was found to be (45/0/0/45) using a carbon fiber fabric, leading to a maximum displacement of 15.27 mm. The introduction of the spar diminished the maximum displacement by 29.7%, while the ribs did not produce a substantial shift in the structural response [32].

In prior research, it was demonstrated that the use of inflatable wings could significantly enhance the portability of small Unmanned Aerial Vehicles (UAVs). The concept of a foam-inflated wing was explored, encompassing a blend of rigid and flexible components, which may potentially lessen the packing and logistical requirements prior to the deployment of a small UAV. The minimization of the wing's packing volume was achieved through the utilization of flexible polyester-film materials for the construction of spars and wing skin. The cylindrical spars were rigidified by the application of expanding foam for deployment, thereby enhancing their resistance to buckling. Rigid ribs, which had been affixed to the spars prior, ensured high shape compliance for the external skin. As a result of the solid rib configuration, the chord length of the wing determined the maximum packing dimension pre-inflation. Testing demonstrated that the hybrid wing's inflation process was straightforward and rapid. The resulting foam-inflated structure was lightweight and could be adapted to the anticipated loads. Moreover, the fundamental ribs maintained high aerodynamic performance, notwithstanding the inflatable characteristics of the hybrid wing structure. The practicality of this hybrid wing structure concept was verified through flight testing [33].

In a previous paper, the exploration of possibilities for simulating composite materials in the SOLIDWORKS environment, along with various aspects of the unmanned aerial vehicle (UAV) design and manufacturing process (using a real airplane model from the Air Cargo Challenge 2013 competition), was presented. The initial section of the paper dealt with various types of composite materials, their mechanical properties, and structures. The process of designing a UAV wing was depicted as a multi-phase task. The subsequent section included numerical analysis related to two composite structure types: laminates and sandwich composites. Variations in displacement and primary stress values (P1, P3) in the aforementioned structures under identical boundary conditions were highlighted. The article concluded with the elaboration of the manufacturing process development [34].

In a previous paper, a terminal guidance control was designed for small fixed-wing unmanned aerial vehicles that have wingspan around 1.5 m was proposed, utilizing a visible light strap-down seeker. The implementation of the system was accomplished using inexpensive, open-source components, costing less than $2000. The system demonstrated feasibility, adaptability, and effectiveness for various types of SUAVs, delivering commendable terminal guidance accuracy (circular error probable = 1.5 m) against a stationary target on the ground. The effects of low-cost and low-precision electrical modules were found to primarily affect terminal guidance information, measurement of SUAV state values, and the system's time-delay. The practical median flow algorithm was examined for target tracking, the attitude pursuit guidance law for terminal guidance control, and the pursuit image frame method for large delay interception to counteract negative influences. Laboratory tests and field flight trials on two different SUAV platforms were utilized to assess the performance and robustness. This paper offers a reliable, efficacious, and tested reference for the evolution of aggressive SUAV for SUAV swarms [35].

The goal of one of the previous papers was to provide guidance through the intricate procedures of design, production, and examination of an electrically propelled, radio-guided aircraft capable of successful take-off, cruising, safe landing, and bearing the maximum payload achievable. The comprehensive process was composed of several stages, including the design phase, structural assessment, performance appraisal, choice of materials, manufacturing, and ultimately, the testing of the aircraft. The final model was constructed with an empty weight and a maximum take-off weight of 15.43 lbs and 33.07 lbs respectively. Moreover, the aircraft had a wingspan of 70.1 inches, a cruising speed of 46 feet per second, and a top speed of 78 feet per second. The total distance required for take-off was recorded to be 100 feet [36].

In previous thesis, the development of the wing structure for a UAV known as Skywalker X8 was documented. An initial model of the UAV was provided and scrutinized to engineer a wing box structure, which was twice as large as the existing model, utilizing eco-friendly technology and lightweight materials. The forces acting upon the UAV were modelled and subsequently assessed using a Computational Fluid Dynamics (CFD) software named Star CCM+. Alterations to the Computer-Aided Design (CAD) model and Finite Element Method (FEM) simulations were executed in Siemens NX. A total of eight combinations of the following five materials were experimented with: carbon fibre reinforced polymer (CFRP), low-density polyethylene (LDPE), polyethylene, polypropylene, and balsa wood. The combination meeting the given requirements most effectively comprised of polypropylene for the wing skin and balsa for the honeycomb structure. This design, weighing 3.576 kg, yielded stress levels of 0.671 MPa, 0.340 MPa, 1 MPa, and 4 MPa for angle of attacks at 1, 2, 3, and 6 degrees respectively. The trailing edge underwent a modification, which involved the addition of a Gurney flap to explore potential improvements in the lift-to-drag ratio. However, it failed to provide the anticipated enhancements and was thus not pursued further [37].

In a previous study, the challenges linked to designing a high-altitude mini–Unmanned Aerial Vehicle (UAV), especially from an aerodynamic standpoint, were highlighted. The mini-UAV being evaluated was a 2 kg class, high-wing, and T-Tail configuration. A comparative analysis of various high lift airfoils was conducted to demonstrate that the choice of an appropriate airfoil for high altitude usage is a significant part of the design process. The study showed that the wing loading of a high-altitude UAV is not solely dependent on-air density variations. The selected high lift, low Reynolds number airfoil was observed to have a marginal impact on the aerodynamic parameters (Cl and Cd) with fluctuations in the Reynolds number. This paper also discussed the variations in performance caused by operating at off-design conditions, such as sea level [38].

Other study focused on the conception, examination, and creation of a hand-launch, fixed-wing unmanned aerial vehicle (UAV), capable of carrying a payload of 0.8. The design procedure entailed conceptual, preliminary, and comprehensive planning. An exploration of the aerodynamic properties over the wing was included in the study to improve the UAV's aerodynamic design. This examination aimed to estimate the optimum gliding ratio to extend the flight mission and achieve the greatest altitude. The simulation was conducted for subsonic flow with a Mach number of 0.04202 (14.3m/s). The UAV's manufacture was carried out utilizing composite materials such as 1mm and 2mm thick glass fiber, 2mm thick carbon fiber, and a carbon rod to attach the empennage to the fuselage. The intricate design was completed in CATIA V5, and the wing's analysis was executed using XFLR and ANSYS (fluent) [39].

The goal of one of previous research was to validate the performance of the wing by analysing its internal structure under maximum lift and inertia force. The wing's reciprocating motion in a stroke was analysed to estimate its peak speed in the stroke as well as its inertia force load when combined with a reciprocating driver. At the highest angle of attack (AoA) and the identified maximum speed, a 3D computational fluid dynamic (CFD) analysis was performed to ascertain the maximum lift and drag. The results from a finite element analysis (FEA) showed acceptable stress levels, indicative of the wing structure's safe load-bearing capacity. This could certify the wing's appropriateness for incorporation into the RA UAV module [40].

The methodology for modelling the nonlinear flight dynamics of BPPT Wulung, a fixed-wing UAV, under varying flight altitude and airspeed conditions was proposed in a previous study, marking an initial step towards designing a nonlinear adaptive controller. The model was cast into 10 degrees-of-freedom (DOF) differential equations configured as strict-feedback systems, segregating the elements of elevator, aileron, rudder, and throttle from the model. The outcomes of the model simulation exposed the behaviour of the Wulung UAV's flight dynamics and also corroborated the concurrence with the real flight test results [41].

A prior article presents an innovative approach that leverages artificial neural networks (ANN) to apply aerodynamic pressures on unmanned aerial vehicles (UAVs) during their design phase. This research primarily aimed to enable a seamless fluid-solid interaction for the structural design of UAVs. By harnessing the capabilities of Computational Fluid Dynamics (CFD), aerodynamic forces were integrated into the UAV's steady-state static design using finite element (FE) analysis. Recognizing the disparities in meshing techniques between CFD and FE tools, the researchers crafted a method with ANNs to formulate precise pressure functions. After training the ANN with aerodynamic data, these functions were instrumental in determining the UAV's structural strength and rigidity. Impressively, the study showcased that ANNs outperformed conventional 3D regression methods in accurately replicating the aircraft's pressure profile [42].

A comprehensive studding was conducted to understand the response of different composite materials when subjected to impact forces. The foundation of the study emphasized that the precision of numerical simulations hinges significantly on well-defined boundary conditions, such as accurate loading conditions and pure mechanical attributes. The research focused on the impact assessment of Carbon, Glass, and Kevlar fiber composites, using FSI analysis. Tools like Ansys Design Modeler played a role in creating the conceptual designs, while the composites were crafted with the ACP tool. The main aim was to identify the most apt material for impact-intensive tasks. Findings from the research suggested that specific composites, notably those derived from Carbon and S-Glass Uni-Directional fibers, were best suited for addressing impact-related challenges, particularly in areas like Unmanned Aerial Vehicles (UAVs) [43].

In a previous study, design variables were rapidly computed to meet the strength and stability conditions, the primary verification parameters for composite wing structure, using a genetic algorithm. An optimization process for variable stiffness stacking, suitable for aircraft wing structure design, was developed. An optimization strategy based on laminate parameters was proposed, considering the stiffness features of the two-dimensional elements employed as design variables. When contrasted with optimization results secured using continuous stiffness optimization as a process function of laminate sequences with genetic algorithms, a sensible stiffness distribution was achieved that complied with crucial guidelines related to individual composite layup designs. The results of the stiffness optimization design were enacted as a finite element model and validated through NASTRAN. The functionality of the stiffness optimization process was showcased by achieving outcomes satisfying the defined response conditions, such as strength and stability, across multiple wing design areas [44].

In previous research, the aerodynamic analysis of unmanned aerial vehicles (UAVs) moving in groups was focused on. The importance of understanding how UAVs move closely to one another was highlighted in the study. Models of a UAV and its propellers were designed using computational fluid dynamics, and turbulence, pressure, and speed changes were investigated. It was discovered that the movement of one UAV in a flock could affect the movement of another. More specifically, unstable motion in one drone could be caused by the aerodynamic effects from a nearby drone. The conclusion drawn from the study was that a certain distance should be maintained between drones moving in groups to reduce these aerodynamic effects. For UAVs that operate on their own, the importance of recognizing and managing their distance from other UAVs was underscored, indicating a need for UAV models to establish their own safe aerodynamic zones [45].

In previous study, the strength and stiffness characteristics of a carbon composite wing belonging to an ultralight unmanned aerial vehicle were investigated, and the results are presented. The wing was made up of foam-core sandwich skins and several spars, each with distinct laminate ply patterns and dimensions of wall thickness. A three-tier whiffletree system was designed and employed to load the wing in accordance with a pull-up-manoeuvre condition. Multiple strain and deflection gauges were utilized to record the static response of the wing at various spanwise and chordwise locations. The wing was loaded incrementally beyond the limit and design ultimate loads until structural failure occurred. A geometric nonlinear finite element model, accounting for the variations in laminate geometry of each component as well as the properties of the adhesively bonded joints in the wing assembly, was developed. With careful alignment of the boundary conditions to those of the experimental setup, the static response of the wing under a simulated whiffletree loading condition was obtained. A strong alignment was found between the experimental observations and the strain and deflection predictions derived from the finite element simulations. Despite its lightness, the wing was discovered to be extremely robust, exhibiting a strength-to-weight ratio exceeding 40 at the point of failure [46].

The focus of this previous research was the structural design methodology for an Unmanned Aerial Vehicle's wing, where computational methods in design were effectively employed.

The strength and stiffness examination of the UAV wing was accomplished through the use of ANSYS, an FEA software. The CAD model on hand and the aerodynamic CFD analysis of the vehicle served as design input. The aerodynamic loads were inflicted on the structure in the form of pressure functions via a novel methodology that harnessed Artificial Neural Networks. The potential effects of variations in geometry, material, and lay-up were also scrutinized to identify the optimal combination that offered superior strength and stiffness while minimizing weight and cost. The final design consisted of a wing with two spars and an entirely composite structure. When compared to a similar aluminium wing, this wing was lighter in weight and had adequate strength to withstand all in-flight load conditions and safety factors [47].

In previous research, the procedure of the UAV wing's structural design, assessment, and optimization for weight reduction was detailed. An optimized semi-monocoque wing structure, encompassing ribs, spars, and skin, was developed with an emphasis on minimizing weight without negatively impacting the strength to weight ratio. Initially, an airfoil of NACA 2412 coordinates was employed in the design of a solid wing surface. Computational Fluid Dynamics (CFD) analysis was then executed to obtain the distribution of pressure across varied wing configurations by adjusting attack angles. Variations in the lift coefficient for distinct attack angles were ascertained from the CFD outcomes. For the structural examination, the pressure fields yielded from the CFD analysis were applied to the structural components. To achieve the targeted performance, the wing was optimized through consideration of multiple scenarios. Findings for the optimized wing facilitated a reduction in wing weight and an increase in the strength to weight ratio. The results indicated a notable advancement compared to the standard model [48].

3. METHODOLOGY

This chapter provides a comprehensive overview of fluid dynamics and its diverse applications. Initially, the focus is on aerodynamics, discussing its foundational principles and its impact on technology and various industries. The chapter then transitions to Computational Fluid Dynamics (CFD), highlighting its significance in analysing fluid behaviours. Key developments, challenges, and the foundational equations, including the Continuity and Navier-Stokes equations, are elaborated upon, emphasizing their role in fluid flow simulations. The topic of Fluid-Structure Interaction (FSI) is introduced, detailing its importance in studying the interactions between structures and their surrounding or internal fluids. Special attention is given to flow-induced instabilities and their relevance in engineering contexts. The chapter concludes with a case study on the Boeing X-45C, illustrating the integration of design principles, aerodynamics, and computational methodologies. The design processes, aided by CAD tools, and the subsequent CFD and FSI analyses are discussed, providing insights into the development and evaluation of advanced aircraft. By the end of this chapter, readers will have a well-rounded understanding of fluid dynamics, its computational aspects, practical implementations, and the ongoing advancements in the domain.

3.1 AERODYNAMICS SCIENCE

3.1.1 Introduction

At the heart of aerodynamics lies the intricate study of gas dynamics, especially when they meet moving solid structures. While many correlate it primarily with the soaring of aircraft, its reach is far more expansive, permeating numerous aspects of our everyday existence. Think about the cars we navigate or the climatic shifts we undergo; aerodynamics fundamentally Molds our comprehension of these phenomena. Tracing its history, the journey of understanding aerodynamics is rich, shaped by the collective endeavours of many visionaries over time. Notable personalities like Ludwig Prandtl have significantly enriched our grasp of this domain. Prandtl underscored that aerodynamics extends beyond mere flight, focusing on a wider range of issues associated with air movement. His enlightening perspectives and others have paved the way for contemporary aerodynamic inquiries, merging theoretical explorations with tangible uses. While the image of an airplane might be the first thing to pop into our minds when thinking of aerodynamics, it's merely a sliver of its vast applicability. Take automobile designs, for example. The contours and frameworks of vehicles are fine-tuned to facilitate ideal airflow, curbing resistance, and amplifying fuel economy. In a similar vein, the engines propelling many of these machines lean on aerodynamic tenets to perfect gas circulation and combustion processes. Beyond the realm of transport, the influence of aerodynamics is evident in energy harnessing. Wind turbines, to cite an instance, are conceptualized using aerodynamic logic to effectively seize wind power. Thrust mechanisms characterizing jet and rocket engines owe their efficiency to aerodynamic principles, guaranteeing prime propulsion and fuel use. In the architectural sphere too, aerodynamics holds significant sway. Systems like HVAC, which regulate temperature and ensure air purity, are steered by aerodynamic rules. Diving deeper, the intellectual allure of aerodynamics is undeniably mesmerizing. This domain harmoniously marries physics, math, and real-world applications, ushering in boundless avenues for inquiry and innovation. The delicate dance of air currents, the subtleties of air turbulence, and the quest to perfect designs for aerodynamic finesse have ceaselessly fascinated and posed challenges for scholars and technologists alike. To encapsulate, aerodynamics isn't merely a branch of science; it's a reflection of human aspiration and creative prowess. Grounded in sophisticated physics, its principles leave a tangible imprint on our daily routines. As humanity continues its quest, be it in crafting ultra-efficient transport modes or venturing into the cosmic expanse, aerodynamics promises to be a pivotal ally in our technological odyssey [49].

3.1.2 Fundamental Concepts

a. Boundary Layer: In the realm of aerospace, the boundary layer holds significant importance, especially in the aerodynamic design of airplane wings, where the primary objective is to minimize drag. By maintaining a laminar boundary layer over extended regions, such as in laminar airfoils, frictional drag can be reduced to approximately half of that observed in conventional airfoils. Techniques like modifying the wing shape for a favorable pressure distribution and employing suction are pivotal in stabilizing the boundary layer. Notably, in transonic regions, interactions between shock waves and the boundary layer intensify, leading to phenomena like the sound barrier, where drag increases substantially near the speed of sound. Beyond the scope of airplanes, boundary layer theory has been adeptly applied to motor vehicle aerodynamics, emphasizing the displacement action of the wake for accurate flow computation. Moreover, during spacecraft re-entry into Earth's atmosphere, addressing significant heat transfer challenges involves intricate calculations of wall heat transfer and the implementation of cooling mechanisms such as transpiration cooling and ablation, with radiation cooling becoming crucial at extremely high temperatures [50].

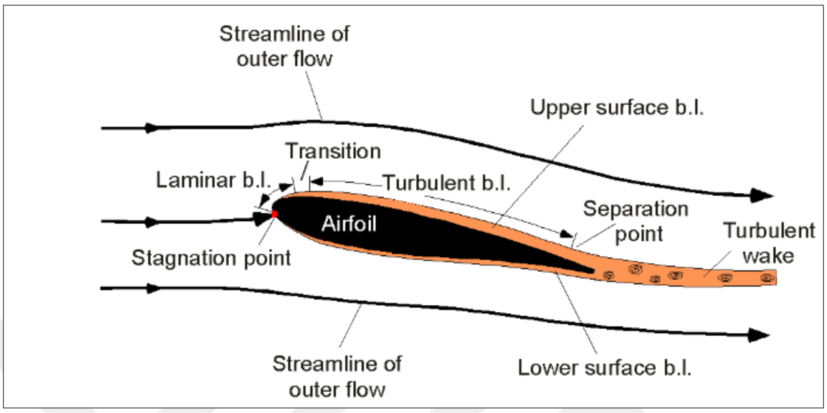

Figure 3.1: Explains Boundary Layer on Airfoil [51].

b. Reynolds Number: The Reynolds number is a fundamental dimensionless parameter in fluid dynamics, profoundly influencing aerospace applications. Micro air vehicles, operating within a low Reynolds number aerodynamic regime (Re < 100,000), contrast starkly with conventional aircraft that fly at Reynolds numbers in the millions. This distinction is crucial as low Reynolds numbers predominantly exhibit laminar flow over airfoils, leading to phenomena such as laminar separation bubbles downstream of the leading edge. Such characteristics result in diminished lift and augmented drag. Furthermore, the drag experienced by objects like spheres in a flow is dominated by flow separation, with the drag coefficient showcasing intriguing variations with the Reynolds number. In the realm of hypersonic vehicles, the Reynolds number plays a role in determining the lift-to-drag ratio, with these vehicles often experiencing extensive laminar flow regions due to the delayed transition to turbulence at high Mach numbers [52]. The Reynolds number could be calculate using equation below [52].

$$Re = \frac{\rho V L}{\mu} \tag{3.1}$$

Where:

ρ : Air density

V : Velocity of the object

L : Characteristic length (like chord length for wings)

μ : Dynamic viscosity of the fluid

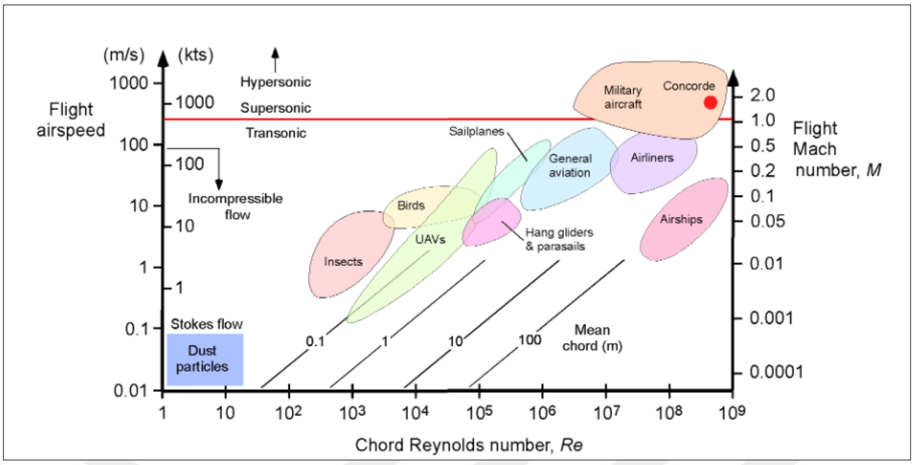

Figure 3.2: Overview of Reynolds and Mach Numbers Observed in Diverse Flight Components [51].

c. Bernoulli's Equation: Bernoulli's equation is a relation between pressure, velocity, and elevation in a frictionless flow. It was initially stated in words by Daniel Bernoulli in 1738 and was later derived in its complete form by Leonhard Euler in 1755. The equation is widely used in fluid mechanics, but it's crucial to understand its limitations. The equation is derived considering an elemental fixed stream tube control volume of variable area A(s). and length ds, where s is the streamline direction. The properties (ρ, V, p) may vary with s and time but are assumed to be uniform over the cross-section A. The equation is given by:

$$\frac{p_1}{\rho} + \frac{1}{2}V_1^{\,2} + gz_1 = \frac{p_2}{\rho} + \frac{1}{2}V_2^{\,2} + gz_2 = constant \qquad (3.2)$$

Where:

p : Pressure.

ρ : Fluid density.

V : Fluid velocity.

g : Acceleration due to gravity

z : Elevation

3.1.3 Aerodynamic Forces

a. Lift Force: Lift is the aerodynamic force created by the pressure and shear stress distributions over the wing surface. This resultant force can be resolved into two forces, parallel and perpendicular to the relative wind. The drag D is defined as the component of the aerodynamic force parallel to the relative wind. The lift L is always defined as the component of the aerodynamic force perpendicular to the relative wind. The angle between the relative wind and the chord line of the aerofoil is the angle of attack α. The lift is mainly due to the imbalance of the pressure distributions over the top and bottom surfaces of the aerofoil. Specifically, the pressure on the top surface of the aerofoil is lower than the pressure on the bottom surface, resulting in lift [52].The lift force could be calculated by equation below [49].

$$L = \frac{1}{2} \times \rho \times V^2 \times S \times C_L \qquad (3.3)$$

Where:

L	:	Lift force.
ρ	:	Air density.
V	:	Velocity of the aircraft relative to the air
S	:	Wing reference area.
C_L	:	Lift coefficient.

The lift coefficient is defined as the aerodynamic lift divided by the dynamic pressure and some reference area. For wings, the convenient reference area S is typically used. The lift coefficient is a function of the Mach number M_∞ and Reynolds number Re. Because ∞ M_∞ and Re are dimensionless, the lift coefficient c l is also dimensionless. The derivation was carried out for an airfoil of a given shape and at a given angle of attack α. If α were to vary, then c l would also vary. Hence, for a given airfoil, the lift coefficient is a function of angle of attack, Mach number, and Reynolds number [52].

b. Drag Force

$$D = \frac{1}{2} \times \rho \times V^2 \times S \times C_D \qquad (3.4)$$

Where:

D : Drag force.

ρ : Air density.

V : Velocity of the aircraft relative to the air

S : Wing reference area.

C_D : Drag coefficient.

The drag coefficient, C_D is a dimensionless quantity that quantifies the drag or resistance of an object in a fluid environment. It represents the drag force on an object moving through a fluid divided by the product of the fluid density, the object's reference area, and the square of the object's velocity [52].

3.2 COMPUTATIONAL FLUID DYNAMICS

3.2.1 Introduction

Originating in the early 1970s, Computational Fluid Dynamics (CFD) was the result of blending physics, numerical mathematics, and computer science to simulate the behaviour of fluid flows. The growth and progress of CFD have been deeply intertwined with the advancements in computer technology. Early on, CFD was primarily used to simulate transonic flows by addressing the non-linear potential equation. As the 1980s rolled in, the industry saw the capability to solve both two-dimensional and, subsequently, three-dimensional Euler equations. With the advent of powerful supercomputers and the introduction of advanced numerical techniques like multigrid, it became possible to simulate non-viscous flows around entire aircraft structures and within complex machinery. By the middle of the decade, there was a noticeable shift towards simulating more intricate viscous flows, primarily governed by the Navier-Stokes equations. This era also marked the rise of advanced turbulence models, prominently featuring direct numerical simulations and large eddy simulations (LES). Towards the end of the 1980s, the industry began tackling flow challenges that required modelling real gases. One of the standout applications from this period was the simulation of three-dimensional hypersonic flows around re-entry vehicles, notably the European HERMES shuttle, utilizing both equilibrium and later, non-equilibrium chemistry models. The importance of simulating combustion and modelling flames grew, especially in the context of creating gas turbines and engines with reduced emissions. The methods to generate grids for these simulations have also seen significant evolution. Starting with basic structured grids, the industry moved to more complex multiblock grids, grids with non-matching interfaces, and eventually the Chimera method. Creating these intricate, multiblock grids for detailed geometries was time-consuming. This challenge paved the way for the creation of unstructured grid generators and solvers, ensuring quicker setup and less manual involvement. In today's context, CFD techniques are a staple in a multitude of sectors, ranging from designing aircraft and machinery to applications in meteorology, ocean studies, and even biological research. CFD has firmly established itself as an indispensable tool for design in engineering and a crucial instrument for research across various scientific domains. However, even with its significant strides, there remain unanswered questions in CFD, especially concerning turbulence, modelling combustion, heat transfer, and optimizing solution methods. The integration of CFD with other scientific areas, such as solid mechanics, is an avenue that still holds much potential. This book is crafted to offer learners a solid grounding in the numerical techniques that underpin contemporary CFD. It also aims to give them practical exposure to modern CFD software. Furthermore, it stands as a valuable guide for professionals and researchers who are either directly involved in CFD or utilize CFD tools in their work [53].

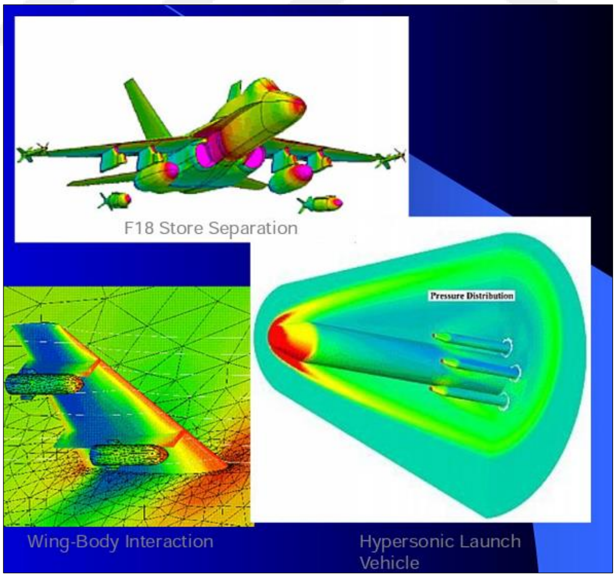

Figure 3.3: Some CFD Applications [54].

3.2.2 Continuity And Navier-Stokes Equations

In the field of Computational Fluid Dynamics (CFD), particularly in aerospace applications, understanding the behaviour of fluid flow is paramount. Two fundamental equations govern this behaviour: the Continuity and Navier-Stokes equations [55].

a. Continuity equation: Ensures the conservation of mass in fluid flow, represented as [56].

$$\nabla \cdot u = 0 \tag{3.5}$$

b. Navier-Stokes equations: Describe the motion of viscous fluid substances. These can be expressed as [56].

$$\frac{\partial u}{\partial t} + u\frac{\partial u}{\partial x} + v\frac{\partial u}{\partial y} = -\frac{1}{\rho}\frac{\partial p}{\partial x} + \nu(\frac{\partial^2 u}{\partial x^2} + \frac{\partial^2 u}{\partial y^2}) \tag{3.6}$$

$$\frac{\partial u}{\partial t} + u\frac{\partial v}{\partial x} + v\frac{\partial v}{\partial y} = -\frac{1}{\rho}\frac{\partial p}{\partial y} + \nu(\frac{\partial^2 v}{\partial x^2} + \frac{\partial^2 v}{\partial y^2}) \tag{3.7}$$

$$\frac{\partial u}{\partial t} + u\frac{\partial w}{\partial x} + v\frac{\partial w}{\partial y} = -\frac{1}{\rho}\frac{\partial p}{\partial z} + \nu(\frac{\partial^2 w}{\partial x^2} + \frac{\partial^2 w}{\partial y^2}) \tag{3.8}$$

Where:

u, v, w	:	velocity components in the x, y, and z directions, respectively.
t	:	time.
ρ	:	fluid density.
ν	:	kinematic viscosity of the fluid.
p	:	pressure field.

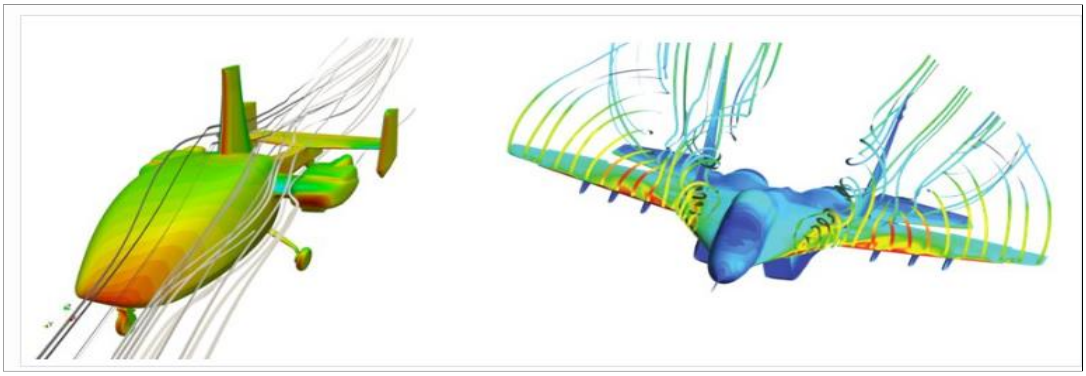

Figure 3.4: CFD-Based Aerodynamic Analysis [54].

c. Fluid-Structure Interaction: Fluid-Structure Interaction (FSI) refers to the dynamic interaction between structures and the fluids that flow around or within them. Structures that meet fluid flow, whether natural or man-made, are always exposed to flow-induced forces and vibrations. These forces can cause self-generated oscillations, also known as instabilities. It is crucial to comprehend these instabilities, particularly when considering the potential for immediate damage. This book focuses on flow-induced instabilities associated with crossflow, which is the flow perpendicular to the structure's long axis. It does not cover every type of FSI, but instead concentrates on specific problems related to cross-flow-induced instabilities. These instabilities and their understanding are of utmost importance in a variety of engineering applications, ranging from heat exchangers to offshore structures, and from tall buildings to submerged pipelines[57].

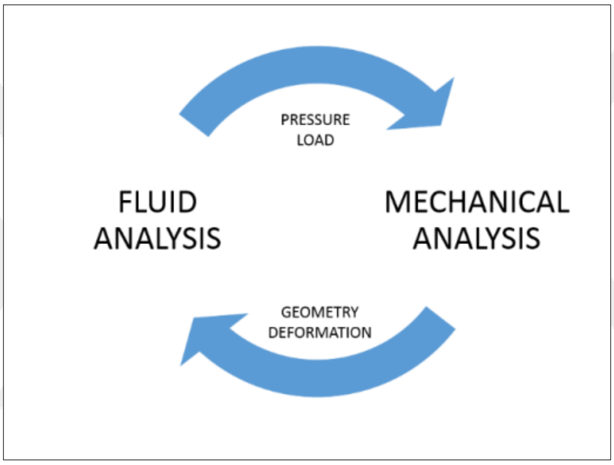

Figure 3.5: Procedure of FSI Analysis [58].

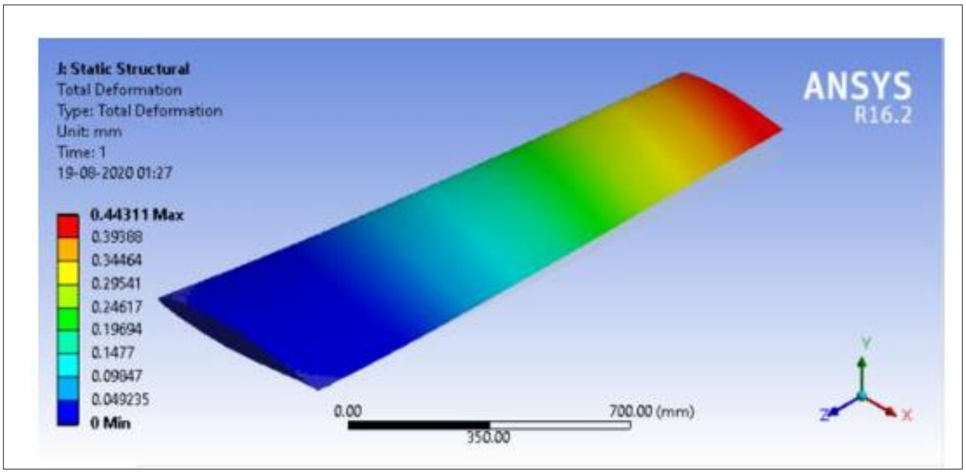

Figure 3.6: Total Deformation Results Got from FSI Analysis [59].

d. Boeing x45c design and analysis.

3.2.3 Introduction

The Boeing X-45C is an emblematic representation of the progress in unmanned combat air vehicles (UCAVs) technology. Stemming from the collaborative efforts of Boeing's Phantom Works division and the U.S. Defense Advanced Research Projects Agency (DARPA), the X-45C was envisioned as the next step in aerial warfare, particularly in high-risk scenarios where manned aircraft might be at greater risk. Characterized by its streamlined, tailless design, it not only reflected advancements in stealth technology but was also indicative of a push towards reduced radar cross-section and increased operational efficiency. Beyond its design, the X-45C was armed with the capability to deploy precision-guided munitions, making it a formidable force in strike missions. However, perhaps the most remarkable feature was its high degree of autonomy. Equipped with state-of-the-art software, the X-45C was designed to conduct intricate operations with minimal human input, while ensuring human operators retained the final decision in critical actions, especially those involving weapon deployment. This aircraft symbolizes a pivotal moment in the evolution of unmanned aerial systems, underscoring the balance between automation and human oversight in modern warfare [60].

Figure 3.7: Boeing X-45C [61].

3.2.4 Boeing X-45C CAD Model Design

To design this plane, there are a lot of programs that can be used, but the SOLIDWORKS software was used due to its ease of use as well as the accuracy of its results.
The figures below show the design of the aircraft, and the dimensions were taken from within the range of dimensions designated for this aircraft from various references.

Table 3.1: Boeing X-45C Dimensions [60].

Parameter	Value
Length	11.89 m
Height	2 m
Wingspan	14.93 m

The Model of the UAV design is in the figures below.

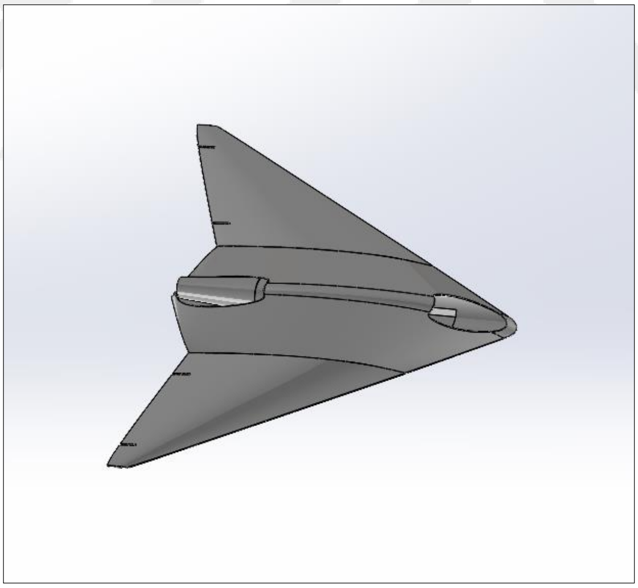

Figure 3.8: Boeing X-45C CAD Model.

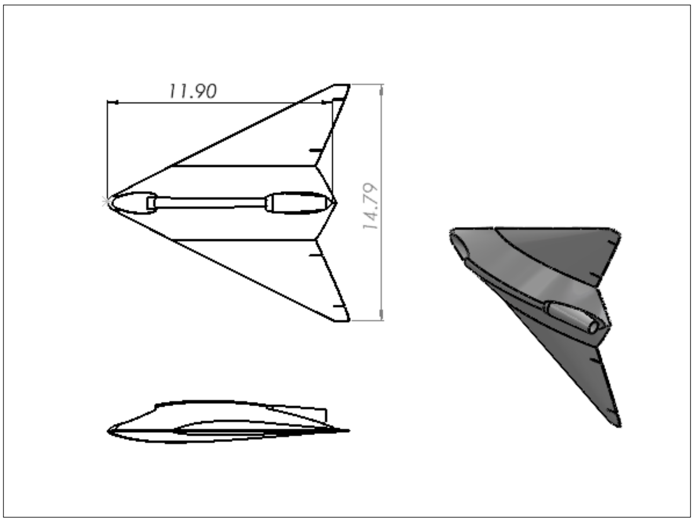

Figure 3.9: Boeing X-45c Drawing that Clarifies Dimensions.

After designing the plane, it was placed in a fluid domain, to complete the CFD Analysis and simulation on it. The domain properties are in the table below.

Table 3.2: Fluid Domain Properties.

Parameter	Value
Domain Length	35 m
Domain Width	40 m
Domain Hight	15 m

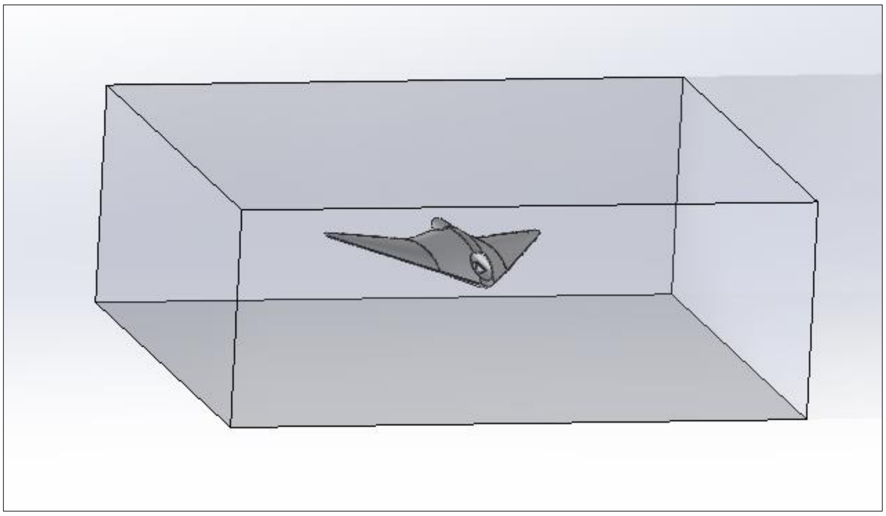

Figure 3.10: Boeing X-45C in Fluid Domain.

a. Boeing X-45C CFD Analysis: After completing the design of the aircraft using SOLIDWORKS, the simulation will now be completed using the ANSYS software, and the UAV will be sent to the ANSYS, either by saving it in a specific format such as (X_t) or by configuration between SOLIDWORKS and ANSYS.

The file is inserted into the geometry in the ANSYS Fluent interface. The first step in the analysis of the CFD on the basis is to conduct the mesh of the existing field, with the focus of the mesh to be of good quality in the presence of the UAV. Mesh settings that were used in the table below.

Table 3.3: Mesh Setting for CFD Analysis.

Parameter	**Value**
Method	Path Independent
Sizing	800 mm

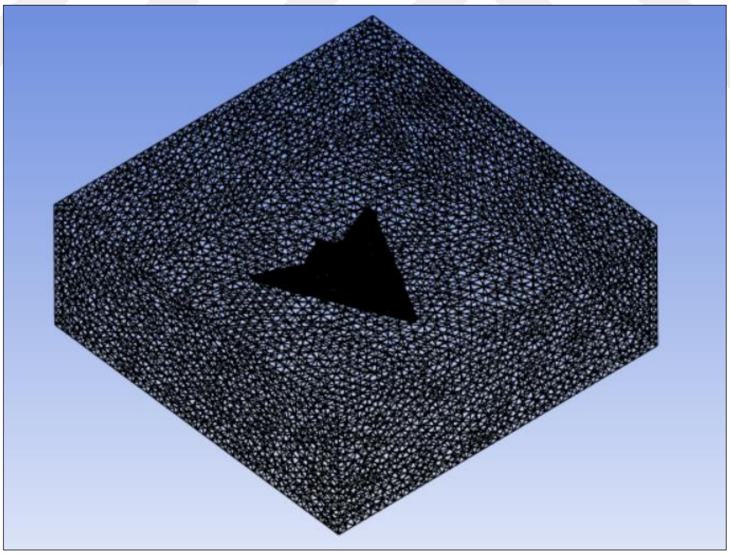

Figure 3.11: Boeing X-45C after Mesh Process for CFD Analysis.

It is also important to name the air inlet and air outlet on the domain that has been placed, where the inlet and outlet, as well as the plane, will be named. And the other parts which are sides and top and bottom walls will be considered as a wall to form a wind tunnel to complete the study.

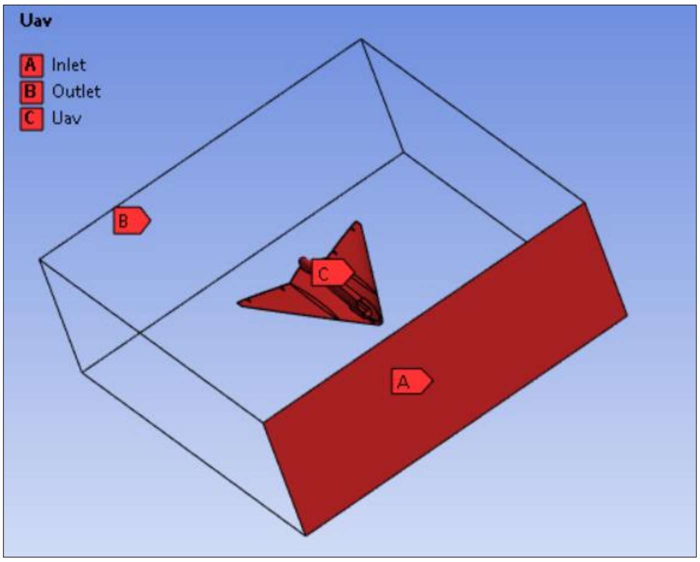

Figure 3.12: Boundary Conditions for CFD Analysis.

After the end of the mesh process, the analysis will be completed on the set-up and the settings that were used in the table below.

Table 3.4: CFD Analysis Setup Settings.

Parameter	Value
Study Type	Pressure Based
Materials	Air
Viscous Model	k-epsilon (2 eq)
Iteration numbers	500
Velocity Inlet	289.2 m/s

The maximum speed of this UAV is 0.85 Mach [60]. that means: Maximum speed (m/s) = 0.85×340.29 (sound speed) = 289.2 m/s. From this analysis, the important contours will be found, as well as the value of drag force, drag coefficient, lift force, and lift coefficient, and they will be reviewed in the next part in the results chapter.

3.2.5 Boeing X-45C FSI Analysis

This analysis begins after the completion of the CFD analysis, where the results of the CFD are linked to the solid of the UAV, where it is imported into the static structure, and the setup of the CFD and the setup of the static structure are linked by a tool called system coupling to transfer the effect of CFD results on the aircraft's solid structure made of aluminum. The same thing will be done for the airframe that was imported into the static structure, where the mesh will be done first, then the boundary condition will be determined as in the table and figures below.

Table 3.5: Mesh Setting for FSI Analysis.

Parameter	Value
Method	Path Conforming
Sizing	100 mm

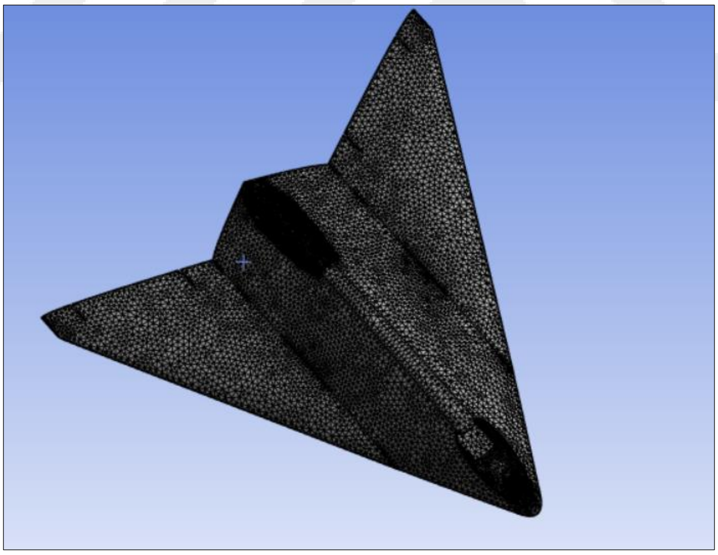

Figure 3.13: Boeing X-45C after Mesh Process for FSI Analysis.

As in any analysis on the ANSYS, the boundary condition must be specified for the FSI analysis, where a specific support must be placed, as well as the fluid solid interface, which is the area on which the forces and effects will be studied, and in this case all the fuselages will be identified.

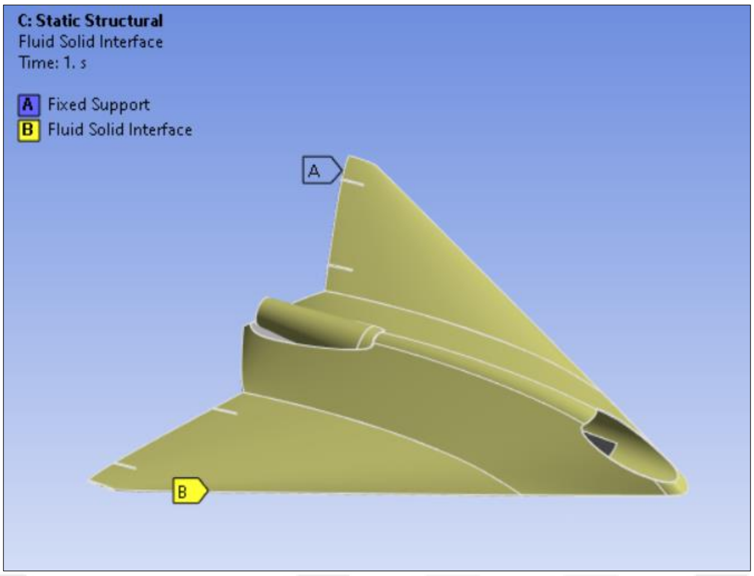

Figure 3.14: Boundary Condition on Boeing X-45C for FSI Analysis.

After that, the results to be found are determined and reviewed in the results chapter, which are the maximum stress, the maximum deformation, the safety coefficient, and the elastic strain. The figure below shows how to connect the CFD analysis to the static structure analysis using the system coupling tool.

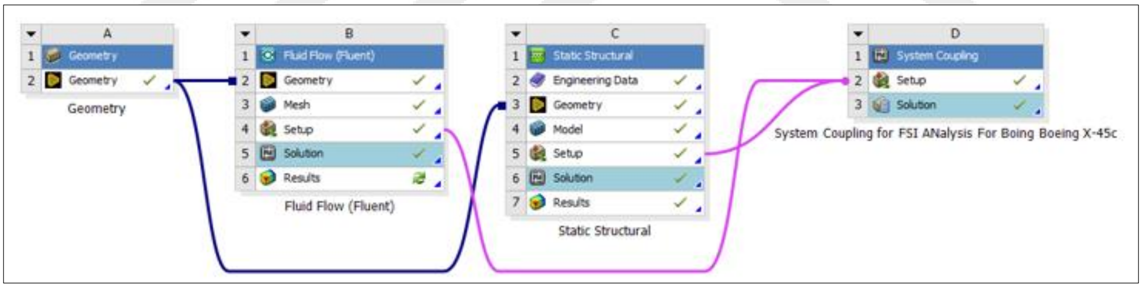

Figure 3.15: Project Schematic for FSI Analysis.

4. RESULTS AND DISSCUSIONS

In this chapter, the results that have been reached will be reviewed. First, the results of the CFD analysis will be reviewed, and then the results of the FSI will be fully reviewed and commented on.

4.1 COMPUTATIONAL FLUID DYNAMICS RESULTS

4.1.1 Drag And Lift Forces

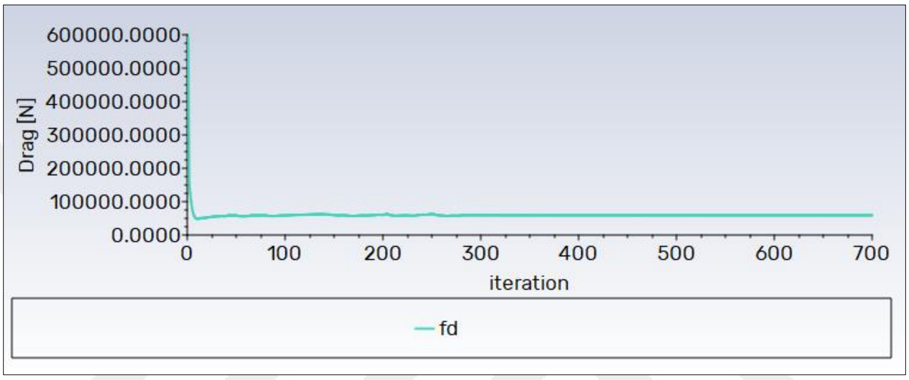

Figure 4.1: Drag Force Values vs Itarations.

The value of the drag force is 61.23 kN.

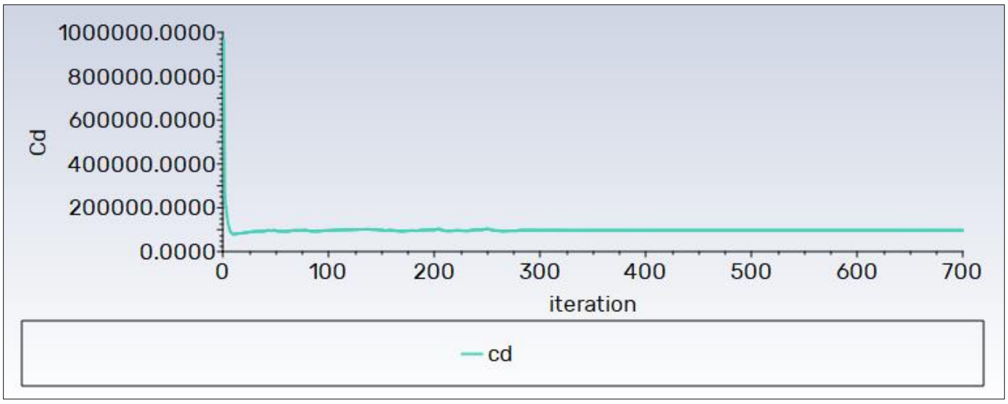

Figure 4.2: Drag Cofficient Values vs Itarations.

The value of the drag cofficent is 93154.

Note that the results were taken after the line between the parameters and iterations was fixed.

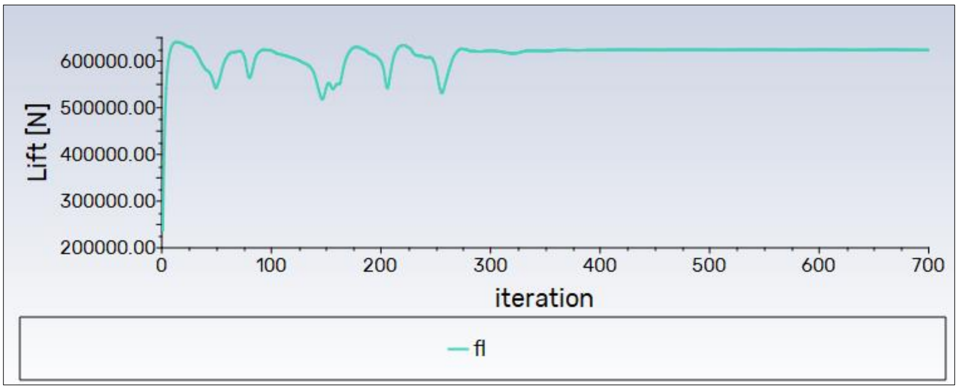

Figure 4.3: Lift Force Values vs Itarations.

The value of the drag force is 625.42 kN.

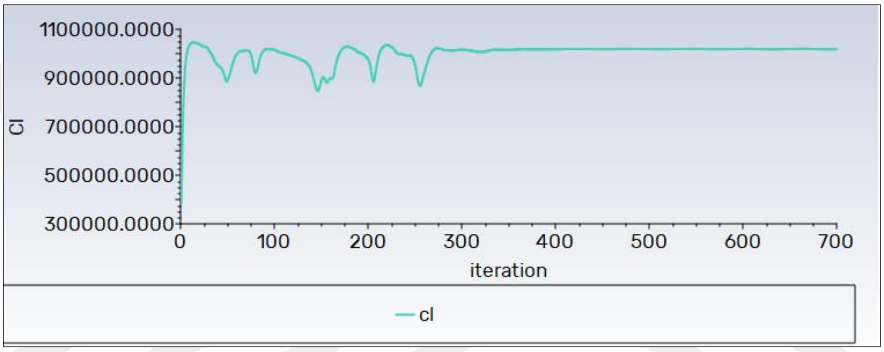

Figure 4.4: Lift Cofficent Values vs Itarations.

The value of the lift cofficent is 994305.

4.1.2 Pressure And Velocity Values ,Contours And Plots

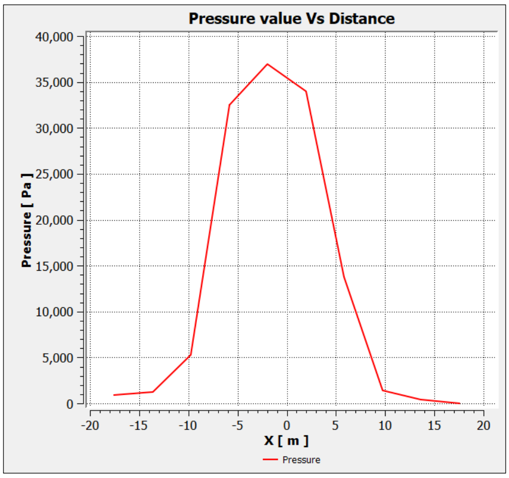

Figure 4.5: Pressure Values vs Domain Distance.

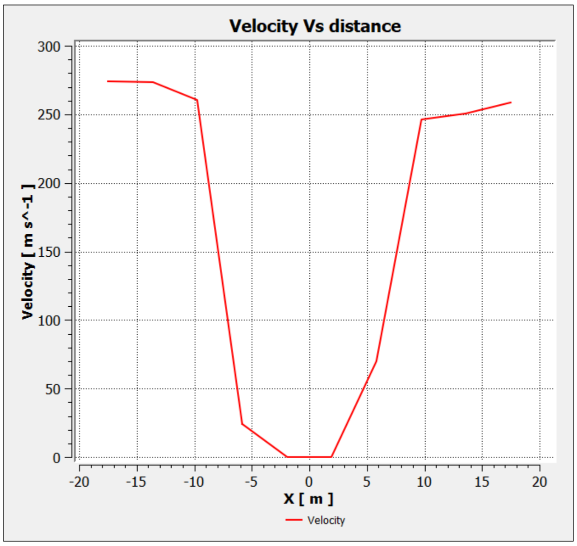

Figure 4.6: Velocity Values vs Domain Distance.

This result is logical based on the Bernoulli equation explained earlier. As the fluid velocity increases, the pressure decreases, and vice versa.

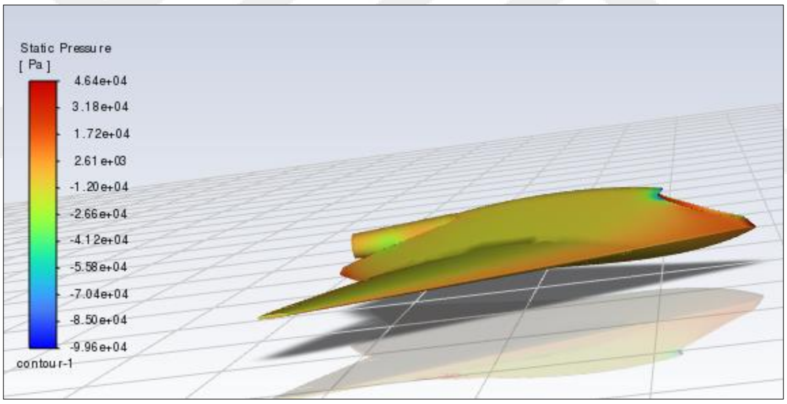

Figure 4.7: Pressure Contours on 3D UAV Model.

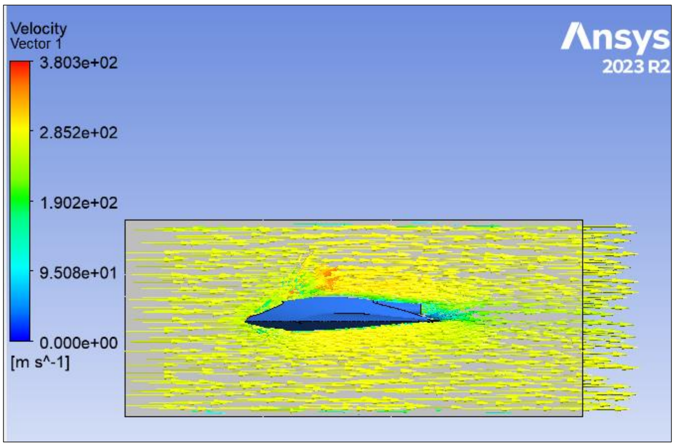

Figure 4.8: Velocity Values as Vectors on 2D Plane on the Mid of UAV Body.

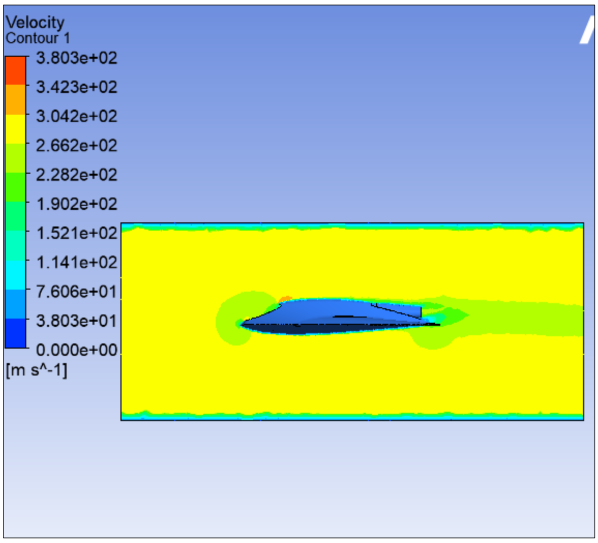

Figure 4.9: Velocity Vectors Contours on 2D Plane on the Mid of UAV Body.

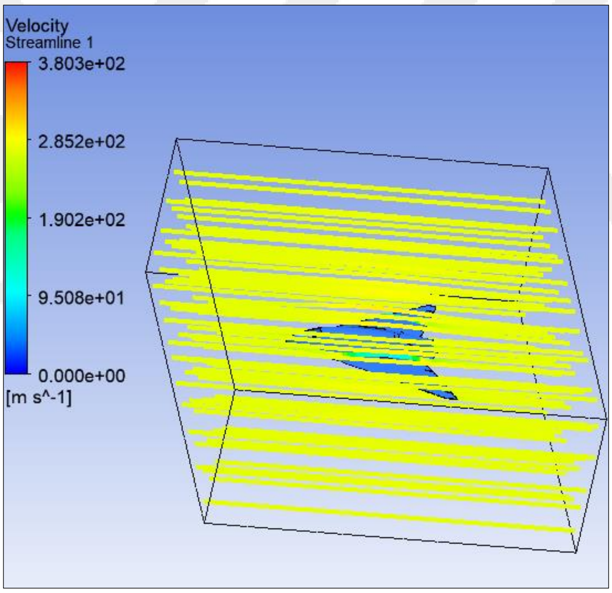

Figure 4.10: Velocity Values as Strem Lines on the Fluid Domain.

From the results above, it is concluded that when the air reaches the plane while it is traveling at its maximum speed, the air speed decreases, and this is logical because it collides with the plane. While the pressure increases as a result of the decrease in speed according to Bernoulli's equation, and as noted, the pressure above the wing is generally negative and precisely, the pressure below the wing is higher from the above pressure, and this is logical according to the science of aviation, and this is what leads to the plane remaining stationary in the sky, and also because the lifting force exceeds the gravitational force many times over

4.2 FLUID-STRUCTURE INTERACTION RESULTS

The FSI results obtained after transferring the effects of air forces to the airframe and the results will be presented in the Static Structure interface.

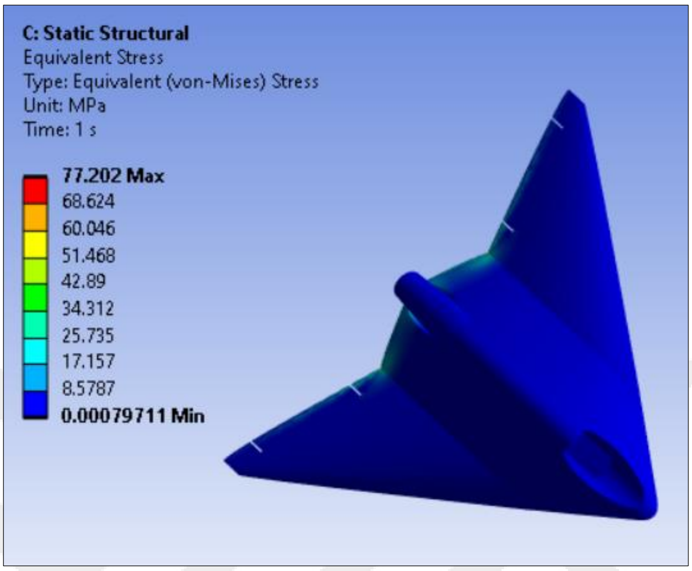

Figure 4.11: Maximum Von-Mises Stress.

The maximum Stress is 77.202 Mpa.

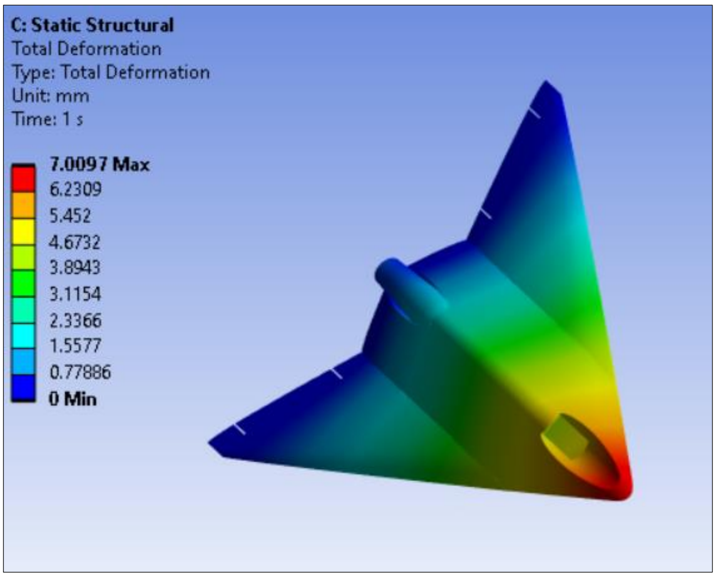

Figure 4.12: Total Deformations.

Total Deformation is 7.0097 mm.

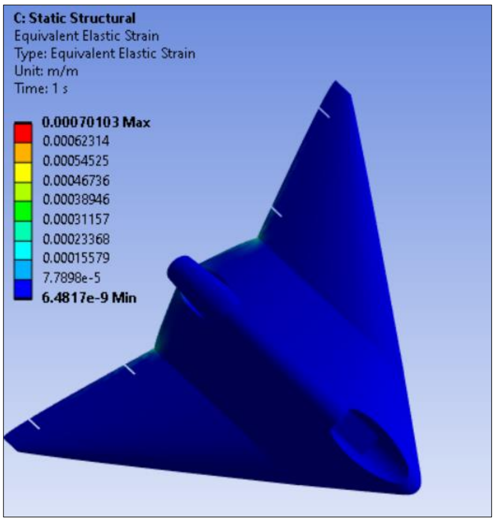

Figure 4.13: Equivelent Elastic Strain.

The Equivalent Elastic Strain is 0.000701.

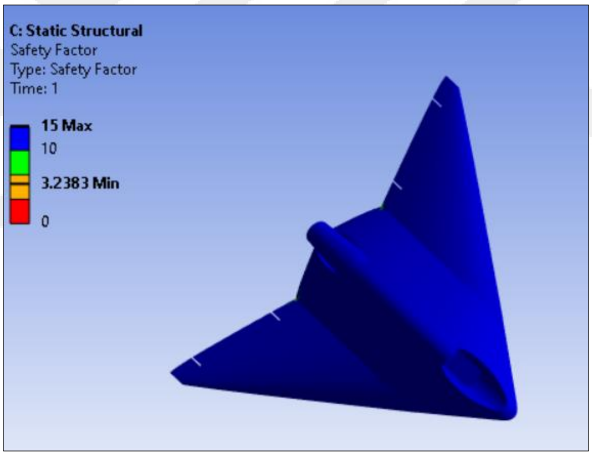

Figure 4.14: Factor of Safety Values.

The value of the safety factor is 3.283 when the plane structure is made from aluminum. So, in this case it will be safe because it is greater than 1.

At the end, The UAV has a drag force of 61.23 kN. This measures the air resistance it faces when flying. Along with this, there's a drag number of 93154. This suggests that some parts of the drone's design might be causing extra drag. On the other hand, the force that helps the drone stay up, called lift, is a strong 625.42 kN. The related lift number is 994305, showing the drone is very good at rising in the air. When comparing drag and lift, it's clear the drone is well-balanced in flight. The relationship between air speed and pressure matches the Bernoulli principle: faster air speed means lower pressure and vice versa. Looking closely, different pressure areas on the 3D drone model can be seen. These areas affect how the drone flies. The flow patterns around the drone give a full view of how it interacts with the air. The highest stress on the drone is 77.202 Mpa. This stress level, along with a bending measure of 7.0097 mm, shows how strong the drone is in different flight situations. There's also a safety value of 3.283 for the drone's structure when it's made from aluminum. This means the drone can handle forces over three times more than what it's designed for without breaking. This is very important for flying machines where safety is a top priority. Overall, the results tell us about the drone's flying strength and give ideas for making its design even better.

5. CONCLUSIONS AND FUTURE WORK

From this study, several key points emerge. Firstly, it's evident that a thorough understanding of computer software is essential. Additionally, anyone using these tools should be well-versed in the topics they aim to design or simulate. This ensures the programs are used effectively and reliably. Generally speaking, as highlighted in the research, this software are based on the finite element method. While this method offers an approximate solution rather than an exact one, using the program properly can yield results that closely mirror real-life scenarios.

The simulation results were logical, whether in terms of pressure readings, velocities, or stress levels. This aircraft is designed to handle pressure at its highest speeds. The identified safety coefficient confirms this, indicating that the aircraft can manage up to three times the maximum force it might face due to speed.

For future studies, it would be beneficial to test the aircraft in real-world conditions, such as in a wind tunnel, maintaining the same dimensions and design specifications as discussed in this research. By doing so, we can compare real-life data with the findings from this study. Additionally, exploring the use of composite materials on the aircraft's body or wings, and then repeating the study, could be valuable. A subsequent comparison between the two sets of findings – one with standard materials and the other with composites – would provide deeper insights.

REFERENCES

[1] J. E. Vance and W. J. Boyne, “Airplane | Definition, Types, Mechanics, & Facts | Britannica,” britannica. Encyclopedia Britannica, Inc, 2023. [Online]. Available: https://www.britannica.com/technology/airplane

[2] S. J. Zaloga, Unmanned Aerial Vehicles: Robotic Air Warfare 1917-2007. Oxford: OSPREY PUBLISHING, 2008.

[3] J. Rennie, “Drone Types: Multi-Rotor, Fixed-Wing, Single Rotor, Hybrid VTOL,” AUAV, 2016. https://www.auav.com.au/articles/drone-types/

[4] Y. Alaiwi and A. Mutlu, “Modelling, Simulation and Implementation of Autonomous Unmanned Quadrotor,” International Journal for Science, Technics and Innovations for the Industry “Machines. Technologies. Materials,” vol. 12, no. 8, pp. 320–325, 2018.

[5] S.Han, “A Guide To The Different Types of Drones & UAS - Everglades University,” Everglades University, 2017. https://www.evergladesuniversity.edu/blog/guide-different-types-drones-unmanned-aerial-systems/

[6] K. Raja Sekar, M. Ramesh, R. Naveen, M. S. Prasath, and D. Vigneshmoorthy, “Aerodynamic design and structural optimization of a wing for an Unmanned Aerial Vehicle (UAV),” IOP Conf Ser Mater Sci Eng, vol. 764, no. 1, 2020, doi: 10.1088/1757-899X/764/1/012058.

[7] I. Uyanik and A. Wesley, “Next generation gas emission monitoring system,” in SPE Middle East Oil and Gas Show and Conference, MEOS, Proceedings, 2019. doi: 10.2118/195015-ms.

[8] K. N. Tahar;, A. Ahmad;, W. A. A. W. M. Akib;, and W. M. N. W. Mohd, “Aerial mapping using autonomous fixed-wing unmanned aerial vehicle,” in IEEE 8th International Colloquium on Signal Processing and its Applications, IEEE, 2012, pp. 164–168. doi: 10.1109/CSPA.2012.6194711.

[9] J. Simsiriwong and R. W. Sullivan, "Vibration Testing of a Full-Scale Carbon Composite Ultralight Unmanned Aerial Vehicle," in 51st AIAA/ASME/ASCE/AHS/ASC Structures, Structural Dynamics, and Materials Conference 18th 12 - 15 April 2010, Orlando, Florida, Aerospace research central, 2010.

[10] F. R. Triputra, R. A. S. Bambang R. Trilaksono, and M. Dahsyat, "Longitudinal Dynamic System Modeling of a Fixed-Wing UAV towards Autonomous Flight Control System Development – A Case Study of BPPT Wulung UAV Platform –," in 2012 International Conference on System Engineering and Technology (ICSET), [IEEE], 2012, pp. 1–6. doi: 10.1109/ICSEngT.2012.6339294.

[11] R. Warsi Sullivan, Y. Hwang, M. Rais-Rohani, and T. Lacy, "Structural analysis and testing of an ultralight unmanned-aerial-vehicle carbon-composite wing," J Aircr, vol. 46, no. 3, pp. 814–820, 2009, doi: 10.2514/1.36415.

[12] W. Grodzki and A. Łukaszewicz, "Design and manufacture of umanned aerial vehicles (UAV) wing structure using composite materials," Materwiss Werksttech, vol. 46, no. 3, pp. 269–278, Mar. 2015, doi: 10.1002/mawe.201500351.

[13] G. Nugroho, A. A. Rafsan Jani, R. R. Trio Sadewo, and M. Satrio, "Manufacturing Process and Flight Testing of an Unmanned Aerial Vehicle (UAV) with Composite Material," Applied Mechanics and Materials, vol. 842, pp. 311–318, Jun. 2016, doi: 10.4028/www.scientific.net/amm.842.311.

[14] E. Esin, "VISION-AIDED LANDING FOR FIXED WING UNMANNED AERIAL VEHICLE," MIDDLE EAST TECHNICAL UNIVERSIT, 2016. doi: 10.13140/RG.2.2.13588.09606.

[15] M. F. Soetanto and R. I. Tritjahjono, "Study the Strength of Material and Composite Structures of Belly-Landing Mini UAV," Applied Mechanics and Materials, vol. 842, pp. 178–185, Jun. 2016, doi: 10.4028/www.scientific.net/amm.842.178.

[16] C. Liu, O. McAree, and W. H. Chen, “Path-following control for small fixed-wing unmanned aerial vehicles under wind disturbances,” International Journal of Robust and Nonlinear Control, vol. 23, no. 15, pp. 1682–1698, Oct. 2013, doi: 10.1002/rnc.2938.

[17] J. Yu, “Design and Optimization of Wing Structure for a Fixed-Wing Unmanned Aerial Vehicle (UAV),” Modern Mechanical Engineering, vol. 08, no. 04, pp. 249–263, 2018, doi: 10.4236/mme.2018.84017.

[18] T. SARAÇYAKUPOĞLU, H. D. DELİBAŞ, and A. D. ÖZÇELİK, “An Experimental Determination and Numerical Analysis of a Loiter Munition Unmanned Aerial Vehicle System,” International Journal of 3D Printing Technologies and Digital Industry, vol. 6, no. 1, pp. 83–101, 2022, doi: 10.46519/ij3dptdi.1083686.

[19] A. V. Azarov, F. K. Antonov, M. V. Golubev, A. R. Khaziev, and S. A. Ushanov, “Composite 3D printing for the small size unmanned aerial vehicle structure,” Compos B Eng, vol. 169, pp. 157–163, Jul. 2019, doi: 10.1016/j.compositesb.2019.03.073.

[20] E. I. Basri et al., “Conceptual design and simulation validation based finite element optimisation for tubercle leading edge composite wing of an unmanned aerial vehicle,” Journal of Materials Research and Technology, vol. 8, no. 5, pp. 4374–4386, Sep. 2019, doi: 10.1016/j.jmrt.2019.07.049.

[21] C. Kim and Y. Lee, “MULTI-DISCIPLINARY DESIGN OPTIMIZATION OF UNMANNED AERIAL VEHICLE,” in Proceedings of the ASME 2011 Pressure Vessels & Piping Division Conference PVP2011 July 17-21, 2011, Baltimore, Maryland, USA, Maryland, 2016, pp. 1–4.

[22] S. H. Son, B. L. Choi, W. J. Won, Y. G. Lee, C. W. Kim, and D. H. Choi, “Wing design optimization for a long-endurance UAV using FSI analysis and the kriging method,” International Journal of Aeronautical and Space Sciences, vol. 17, no. 3, pp. 423–431, 2016, doi: 10.5139/IJASS.2016.17.3.423.

[23] R. Vijayakumar and S. K. Maharana, "Experimental Characterization Of Graphene-Based Polymer Matrix Composites For An Unmanned Aerial Vehicle," International Journal of Materials Engineering and Technology, vol. 18, no. 1, pp. 1–16, Apr. 2019, doi: 10.17654/mt018010001.

[24] C. Cruzatty, E. Sarmiento, E. Valencia, and E. Cando, "Design methodology of a UAV propeller implemented in monitoring activities," Mater Today Proc, vol. 49, pp. 115–121, 2022, doi: 10.1016/j.matpr.2021.07.481.

[25] B. Tamang and I. B. Ghimire, "Design And Fluid-Structure Interaction Study of a Wing Structure for a Medium-Range UAV," TRIBHUVAN UNIVERSITY, 2023.

[26] M. C. Haupt, K. Lindhorst, and P. Horst, "Interfacing MSC nastran to the CFD-Solver DLR-Tau for unsteady FSI analyses with nonlinear aircraft structures," in AeroStruct: Enable and Learn How to Integrate Flexibility in Design, 2018, pp. 155–171. doi: 10.1007/978-3-319-72020-3_10.

[27] F. life estimation of fixed-wing unmanned aerial vehicle engine by grey Forecasting, "Fatigue life estimation of fixed-wing unmanned aerial vehicle engine by grey forecasting," Measurement and Control, vol. 54, no. 5–6, pp. 799–810, May 2020, doi: 10.1177/0020294020915215.

[28] K. Das Patel and B. S. Kumar Karuparthi, "Design, Performance Analysis of Wing, and Manufacturing of Fixed Wing Hand Launch Unmanned Aerial Vehicle," International Journal of Engineering Applied Sciences and Technology, vol. 5, no. 9, pp. 223–241, 2021, doi: 10.33564/ijeast.2021.v05i09.038.

[29] F. R. Triputra, B. R. Trilaksono, T. Adiono, R. A. Sasongko, and M. Dahsyat, "Nonlinear Dynamic Modeling of a Fixed-Wing Unmanned Aerial Vehicle: a Case Study of Wulung," Journal of Mechatronics, Electrical Power, and Vehicular Technology, vol. 6, no. 1, pp. 19–30, Jul. 2015, doi: 10.14203/j.mev.2015.v6.19-30.

[30] Z. Siddiqi and J. W. Lee, "A computational fluid dynamics investigation of subsonic wing designs for unmanned aerial vehicle application," Proc Inst Mech Eng G J Aerosp Eng, vol. 233, no. 15, pp. 5543–5552, 2019, doi: 10.1177/0954410019852553.

[31] R. Ramamurti, J. D. Geder, K. Viswanath, R. Lohner, and O. Soto, "Coupled CFD, Structure and Control Tool for Simulation of Flapping Wing Analysis," 2016.

[32] A. Felipe, C. Rivera, J. Sebastian, L. Becerra, J. Rodriguez-Ferreira, and M. Martínez, "Structural analysis of an unmanned aerial vehicle wing made of composite materials," Scientia et Technica, vol. 26, no. 3, p. 13, 2021, doi: 10.22517/23447214.24535.

[33] G. Bramesfeld and R. Prinster, "Design and testing of foam-inflated wings for small unmanned aerial vehicles," J Unmanned Veh Syst, vol. 3, no. 4, pp. 176–191, 2015, doi: 10.1139/juvs-2014-0018.

[34] W. Grodzki and A. Łukaszewicz, "Design and manufacture of umanned aerial vehicles (UAV) wing structure using composite materials," Materwiss Werksttech, vol. 46, no. 3, pp. 269–278, Mar. 2015, doi: 10.1002/mawe.201500351.

[35] Y. Yang et al., "Design, implementation, and verification of a low-cost terminal guidance system for small fixed-wing UAVs," J Field Robot, vol. 38, no. 5, pp. 801–827, Aug. 2021, doi: 10.1002/rob.22012.

[36] M. El Adawy et al., "Design and fabrication of a fixed-wing Unmanned Aerial Vehicle (UAV)," Ain Shams Engineering Journal, vol. 14, no. 9, Sep. 2023, doi: 10.1016/j.asej.2022.102094.

[37] S. Rahman and A. Ranganathan, "Conceptual design and construction of a UAV wing structure," SCI KTH, 2020.

[38] H. Sharma, C. S. Suraj, R. Antony, G. Ramesh, S. Ahmed, and P. Narayan, "Design of a High-Altitude Fixed Wing Mini UAV-Aerodynamic Challenges," National Aerospace Laboratories Institutional Repository, 2013.

[39] K. Das Patel and B. S. Kumar Karuparthi, "DESIGN, PERFORMANCE ANALYSIS OF WING, AND MANUFACTURING OF FIXED WING HAND LAUNCH UNMANNED AERIAL VEHICLE," International Journal of Engineering Applied Sciences and Technology, vol. 5, no. 9, pp. 233–241, Jan. 2021, doi: 10.33564/ijeast.2021.v05i09.038.

[40] J. O. Imumbhon, M. Landazuri, and Y. Cao, “Structural and CFD analyses of a reciprocating-airfoil (RA) driven UAV wing under maximum lift and inertia forces,” Drone Systems and Applications, vol. 10, no. 1, pp. 287–308, Jan. 2022, doi: 10.1139/dsa-2021-0043.

[41] F. R. Triputra, B. R. Trilaksono, T. Adiono, R. A. Sasongko, and M. Dahsyat, “Nonlinear Dynamic Modeling of a Fixed-Wing Unmanned Aerial Vehicle: a Case Study of Wulung,” Journal of Mechatronics, Electrical Power, and Vehicular Technology, vol. 6, no. 1, pp. 19–30, Jul. 2015, doi: 10.14203/j.mev.2015.v6.19-30.

[42] F. Mazhar, A. M. Khan, I. A. Chaudhry, and M. Ahsan, “On using neural networks in UAV structural design for CFD data fitting and classification,” Aerosp Sci Technol, vol. 30, no. 1, pp. 210–225, 2013, doi: 10.1016/j.ast.2013.08.005.

[43] M. Ramesh et al., “Impact behavioral studies on various composite materials using Fluid-Structure interaction (FSI),” Mater Today Proc, vol. 51, pp. 1134–1140, 2021, doi: 10.1016/j.matpr.2021.07.112.

[44] J. H. Jang and S. H. Ahn, “Optimum Design of UAV Wing Skin Structure with a High Aspect Ratio Using Variable Laminate Stiffness,” Applied Sciences (Switzerland), vol. 12, no. 19, Oct. 2022, doi: 10.3390/app12199436.

[45] M. Atmaca, B. Çetin, and E. Yılmaz, “CFD analysis of unmanned aerial vehicles (UAV) moving in flocks,” Acta Phys Pol A, vol. 135, no. 4, pp. 694–696, 2019, doi: 10.12693/APhysPolA.135.694.

[46] R. Warsi Sullivan, Y. Hwang, M. Rais-Rohani, and T. Lacy, “Structural analysis and testing of an ultralight unmanned-aerial-vehicle carbon-composite wing,” J Aircr, vol. 46, no. 3, pp. 814–820, 2009, doi: 10.2514/1.36415.

[47] F. Mazhar and A. M. Khan, “STRUCTURAL DESIGN OF A UAV WING USING FINITE ELEMENT METHOD,” in 51st AIAA/ASME/ASCE/AHS/ASC Structures, Structural Dynamics, and Materials Conference
 18th, 2010.

[48] K. Raja Sekar, M. Ramesh, R. Naveen, M. S. Prasath, and D. Vigneshmoorthy, "Aerodynamic design and structural optimization of a wing for an Unmanned Aerial Vehicle (UAV)," in IOP Conference Series: Materials Science and Engineering, Institute of Physics Publishing, Mar. 2020. doi: 10.1088/1757-899X/764/1/012058.

[49] J. D. Anderson, Fundamentals of Aerodynamics, 6th ed. New York: Mc Hall Eduication, 2016.

[50] H. Schlichting and K. Gersten, Boundary-Layer Theory, 9th ed. Berlin: Springer Berlin Heidelberg, 2016.

[51] J. G. Leishman, Introduction to Aerospace Flight Vehicles, 1st ed. Florida: Embry-Riddle Aeronautical University, Hunt Library, 2022.

[52] Jr. John D. Anderson and P. Emeritus, Introduction to Flight. New York: McGraw-Hill Education, 2016.

[53] J. BLAZEK, Computational fluid dynamics principles and applications. Oxford OX5: Elsevier, 2015.

[54] T. Xing and F. Stern, "Introduction to computational fluid dynamics," Iowa, 2012. doi: 10.1017/CBO9780511808975.

[55] C. Pozrikidis, Introduction to Theoretical and Computational Fluid Dynamics. Oxford: Oxford University Press Oxford, 2011.

[56] B. R. Munson, T. H. Okiishi, W. W. Huebsch, and A. P. Rothmayer, Fundamentals of fluid mechanics. New York: John Wiley and Sons Inc, 2013. doi: 10.1201/b11709-7.

[57] M. P. Pa¨ıdoussis, S. J. Price, and E. de Langre, Fluid-Structure Interactions CROSS-FLOW-INDUCED INSTABILITIES. Cambridge: Cambridge University Press, 2010.

[58] N. Yilmaz and N. Görener, “Comparison on Hydrodynamic Behavior of Shape-Adaptive and Rigid Marine Propellers,” in The 2nd International Symposium on Naval Architecture and Maritime, 2014, pp. 1–11. [Online]. Available: https://www.researchgate.net/publication/280511221

[59] B. E. S. Srividhya, (Ph.D) K.Nehru, M.Tech, and M. T. M.Subramanian, “Fluid-Structure Interaction Study on an Aircraft wing model using ANSYS Coupling system,” Int J Eng Res Appl, vol. 10, no. 9, pp. 21–32, 2020, doi: 10.9790/9622-1009032132.

[60] K. M. Claffy, “Joint Unmanned Combat Air System Matching Mission Requirements, Performance Capabilities, and Critical Aviation Systems,” University of Tennessee, Knoxville, 2005.

[61] A. Parsch, “Boeing X-45 / X-46,” Directory of U.S. Military Rockets and Missiles, 2007. https://www.designation-systems.net/dusrm/app4/x-45.html